ELSEVIER

Contents lists available at ScienceDirect

Acta Biomaterialia

journal homepage: www.elsevier.com/locate/actbio



Full length article

Electrospun fiber-mediated delivery of neurotrophin-3 mRNA for neural tissue engineering applications



Devan L. Puhl^{a,b}, Jessica L. Funnell^{a,b}, Tanner D. Fink^{b,c}, Anuj Swaminathan^{a,b}, Martin Oudega^{d,e,f,g}, R. Helen Zha^{b,c}, Ryan J. Gilbert^{a,b,*}

- ^a Department of Biomedical Engineering, Rensselaer Polytechnic Institute, Troy, NY, USA
- ^b Center for Biotechnology and Interdisciplinary Studies, Rensselaer Polytechnic Institute, Troy, NY, USA
- ^c Department of Chemical and Biological Engineering, Rensselaer Polytechnic Institute, Troy, NY, USA
- ^d Shirley Ryan AbilityLab, Chicago, IL, USA
- ^e Department of Physical Therapy and Human Movement Sciences, Northwestern University, Chicago, IL, USA
- f Department of Neuroscience, Northwestern University, Chicago, IL, USA
- g Edward Hines Jr VA Hospital, Hines, IL, USA

ARTICLE INFO

Article history: Received 28 August 2022 Revised 30 October 2022 Accepted 15 November 2022 Available online 21 November 2022

Keywords: Electrospinning mRNA therapeutics Gene delivery Nerve regeneration Neurotrophins Biomaterials

ABSTRACT

Aligned electrospun fibers provide topographical cues and local therapeutic delivery to facilitate robust peripheral nerve regeneration. mRNA delivery enables transient expression of desired proteins that promote axonal regeneration. However, no prior work delivers mRNA from electrospun fibers for peripheral nerve regeneration applications. Here, we developed the first aligned electrospun fibers to deliver pseudouridine-modified (Ψ) neurotrophin-3 (NT-3) mRNA (Ψ NT-3mRNA) to primary Schwann cells and assessed NT-3 secretion and bioactivity. We first electrospun aligned poly(L-lactic acid) (PLLA) fibers and coated them with the anionic substrates dextran sulfate sodium salt (DSS) or poly(3.4-dihydroxy-L-phenylalanine) (pDOPA). Cationic lipoplexes containing ΨNT-3mRNA complexed to JetMESSENGER® were then immobilized to the fibers, resulting in detectable ΨNT -3mRNA release for 28 days from all fiber groups investigated (PLLA+mRNA, 0.5DSS4h+mRNA, and 2pDOPA4h+mRNA). The 2pDOPA4h+mRNA group significantly increased Schwann cell secretion of NT-3 for 21 days compared to control PLLA fibers (p < 0.001 - 0.05) and, on average, increased Schwann cell secretion of NT-3 by ≥ 2 -fold compared to bolus mRNA delivery from the 1µgBolus+mRNA and 3µgBolus+mRNA groups. The 2pDOPA4h+mRNA fibers supported Schwann cell secretion of NT-3 at levels that significantly increased dorsal root ganglia (DRG) neurite extension by 44% (p < 0.0001) and neurite area by 64% (p < 0.001) compared to control PLLA fibers. The data show that the 2pDOPA4h+mRNA fibers enhance the ability of Schwann cells to promote neurite growth from DRG, demonstrating this platform's potential capability to improve peripheral nerve regeneration.

Statement of significance

Aligned electrospun fibers enhance axonal regeneration by providing structural support and guidance cues, but further therapeutic stimulation is necessary to improve functional outcomes. mRNA delivery enables the transient expression of therapeutic proteins, yet achieving local, sustained delivery remains challenging. Previous work shows that genetic material delivery from electrospun fibers improves regeneration; however, mRNA delivery has not been explored. Here, we examine mRNA delivery from aligned electrospun fibers to enhance neurite outgrowth. We show that immobilization of NT-3mRNA/JetMESSENGER® lipoplexes to aligned electrospun fibers functionalized with pDOPA enables local, sustained NT-3mRNA delivery to Schwann cells, increasing Schwann cell secretion of NT-3 and enhancing DRG neurite outgrowth. This study displays the potential benefits of electrospun fiber-mediated mRNA delivery platforms for neural tissue engineering.

Published by Elsevier Ltd on behalf of Acta Materialia Inc.

^{*} Corresponding author at: Center for Biotechnology and Interdisciplinary Studies, Rensselaer Polytechnic Institute, 1623 15th Street, Troy, NY, 12180, USA. E-mail address: gilber2@rpi.edu (R.J. Gilbert).

1. Introduction

Peripheral nervous system (PNS) injury resulting from disease or trauma impacts over 20 million individuals in the United States alone and can significantly reduce the patient's quality of life [1]. Recovery from PNS injury is often incomplete due to limited regeneration of damaged peripheral axons and deficient reinnervation of surrounding tissues [2,3]. A complete nerve transection injury gap larger than 1 cm typically requires surgical placement of a bridging graft to support axon regeneration and functional recovery [4]. A nerve autograft or allograft are the gold standard surgical options to bridge a large injury gap in a peripheral nerve [5]. However, aligned electrospun fiber-containing artificial nerve grafts serve as an alternative approach to bridge large injury gaps with the potential to overcome the limitations faced by autografts and allografts [4–7]. The aligned fibers provide topographical features that mimic the native peripheral nerve extracellular matrix (ECM) and can be engineered to locally deliver therapeutics such as small molecule drugs, proteins, and nucleic acids over an extended duration to support robust axon regeneration [5,8-12].

Delivery of neurotrophic factor proteins from biomaterials following nervous system injury is of interest due to their known benefits on the regeneration process [13–22]. Neurotrophin-3 (NT-3) is a neurotrophic protein that binds to tyrosine kinase (Trk) receptors present on cells throughout the PNS, including Schwann cells and dorsal root ganglia (DRG) neurons [23–26]. This enables NT-3 to elicit a broad range of responses *in vitro* and *in vivo*, such as increasing Schwann cell migration, mediating Schwann cell myelination, enhancing neurite outgrowth from DRG explants, and improving sensory axon regeneration [17,18,27–39]. However, the use of NT-3 as a clinical therapeutic is limited by its short half-life [36,40]. Alternatively, viral or non-viral DNA or RNA delivery can induce local expression of the desired protein [28,36,41–46].

Synthetic messenger RNA (mRNA) delivery offers a non-viral approach to induce transient expression in the cytosol, removing the risk of insertional mutagenesis and improving the transfection efficiency of hard-to-transfect primary cells compared to DNA-based gene therapies [47-50]. The instability and immunogenicity of mRNA have slowed the progression of mRNA therapeutics to the clinic [47]. However, the use of cationic lipid- and polymer-based gene delivery vehicles and incorporation of optimized capping structures like anti-reverse cap analog (ARCA) and modified nucleotides like pseudouridine-5'-triphosphate (Ψ) improve the delivery efficiency of bioactive mRNA and subsequent translation into the desired protein while reducing the risk of a severe immune response to the foreign genetic material [48,51– 56]. Synthetic mRNAs have been successfully delivered via systemic and local injection to increase the production and secretion of neurotrophic factors [43-46]. Still, the limited success of mRNA therapeutics in tissue engineering and regenerative medicine is due, in part, to the challenge of delivering an efficacious dose of mRNA to the target location to induce sustained secretion of the desired protein for the optimal duration [50,57]. Electrospun fiber-based drug depots enable local, sustained, non-viral delivery of genetic material in the forms of plasmid DNA, small interfering RNA (siRNA), and microRNA (miRNA) while also providing structural support and guidance cues to enable robust nerve regeneration [11,12,58-61]. However, mRNA delivery from electrospun fibers to improve neurite outgrowth or axon regeneration via production of neurotrophic factors has yet to be explored.

Poly(L-lactic acid) (PLLA) is an FDA-approved material commonly used to fabricate electrospun fibers for neural repair due to its biocompatibility and slow biodegradability [62–64]. Anionic surface coatings like poly(3,4-dihydroxy-L-phenylalanine) (pDOPA) and dextran sulfate sodium salt (DSS) have been employed to functionalize the electrospun fiber surface and improve immobilization

of biologics for local, sustained delivery [12,61,65–71]. pDOPA possesses carboxyl groups and reactive o-quinones that support the immobilization of cationic delivery vehicles carrying genetic material through a variety of possible physical and chemical interactions, including electrostatic interactions, hydrophobic interactions, hydrogen bonding, or Shiff base or Michael addition reactions, depending on the surface chemistry of the gene delivery vehicle [12,61,65–70]. DSS possesses sulfonate groups and has been deposited onto electrospun fibers to enable immobilization of a cationic enzyme via electrostatic interactions [71]. However, DSS has yet to be employed to immobilize genetic material to the fiber surface.

Here, we aimed to develop the first aligned electrospun fiber platform that delivers modified mRNA encoding NT-3 to 1) sustain local delivery of mRNA, 2) induce secretion of NT-3 protein from primary rat Schwann cells, and 3) enhance neurite outgrowth from rat DRG explants. First, we synthesized pseudouridine-5'triphosphate (Ψ)-modified mRNA encoding NT-3 (Ψ NT-3mRNA). Next, we fabricated aligned PLLA electrospun fibers and functionalized the fiber surface with a pDOPA or DSS coating. We then complexed the WNT-3mRNA to the cationic delivery vehicle JetMESSENGER® to form lipoplexes and immobilized the Ψ NT-3mRNA/JetMESSENGER® lipoplexes to the functionalized electrospun fiber platforms. Finally, we investigated the ability of the ΨNT-3mRNA/JetMESSENGER®-loaded aligned electrospun fiber platforms to induce NT-3 protein secretion from rat Schwann cells and subsequently assessed whether increased NT-3 secretion from Schwann cells promoted neurite outgrowth from rat DRG explants. This study introduces an approach that combines sustained delivery of mRNA with topographical guidance cues to stimulate and guide neurite outgrowth and serves as a basis for future construction and in vivo testing of mRNA-loaded, electrospun fibercontaining artificial nerve grafts.

2. Materials and methods

2.1. Materials

All information regarding the materials, instruments, and software used is included in **Table S1** and **Table S2**.

2.2. ΨNT-3mRNA synthesis

 Ψ NT-3mRNA was synthesized in-house using standard molecular biology techniques described in detail in the supplementary methods. Briefly, a pcDNA3.1(+) expression vector encoding rat NT-3 was expanded in bacteria and then isolated and purified via a maxi-prep. Next, the pcDNA3.1(+)_NT-3 was linearized, and the template DNA was amplified using standard polymerase chain reaction (PCR) techniques. Finally, Ψ -modified, anti-reverse cap analog (ARCA)-capped mRNA encoding NT-3 was synthesized via *in vitro* transcription and purified using spin columns. The Ψ NT-3mRNA quality and bioactivity were evaluated via a bioanalyzer and enzyme-linked immunosorbent assay (ELISA), respectively.

2.3. Lipoplex formation and characterization

The mRNA/JetMESSENGER® lipoplexes were formed according to the JetMESSENGER® manufacturer's protocol. Briefly, anionic Ψ NT-3mRNA and cationic JetMESSENGER® were complexed at a mass-to-volume ratio of 1 μ g Ψ NT-3mRNA to 2 μ L JetMESSENGER® (1:2 w/v) in the provided mRNA buffer. The solution was mixed thoroughly and incubated for 15 min at room temperature before use. The hydrodynamic size, polydispersity index, and charge of the formed mRNA lipoplexes were evaluated by an Anton Paar Litesizer TM 500 using dynamic light scattering (DLS) and

measuring the zeta potential of particles in suspension described in detail in the supplementary methods. Three solutions of each mRNA type were prepared and analyzed (n = 3).

Commercially produced CleanCap® Enhanced Green Fluorescent Protein mRNA (eGFPmRNA), which is similar in size to the Ψ NT-3mRNA (\sim 1 kb), was complexed to JetMESSENGER® and characterized in the same manner described above. eGFPmRNA/JetMESSENGER® lipoplexes were used to conduct bolus transfection efficiency experiments and the eGFPmRNA immobilization pilot study for preliminary investigation of mRNA-loaded electrospun fiber design detailed in the supplementary methods and results.

2.4. Film casting and electrospinning

PLLA films and aligned PLLA fibers were fabricated onto glass coverslips using drop-casting and electrospinning techniques described previously [72]. Briefly, A 4% (w/w) solution of PLLA in chloroform was prepared, and 50 μL or 300 μL of the solution was drop cast evenly onto 15 mm x 15 mm or 24 mm x 50 mm glass coverslips, respectively. The 15 mm x 15 mm films were used for contact angle characterization or before electrospinning fibers to secure the fibers to the coverslip and ensure that cells cultured onto the fibers only encountered one material type. The 24 mm x 50 mm films were used for zeta potential characterization. Next, A 12% (w/w) solution of PLLA in chloroform was prepared and poured into a 5 mL syringe with a 22 G x 1 1/2 inch needle and loaded into a syringe pump. The 15 mm x 15 mm PLLA film-coated coverslips were attached to a grounded wheel (1 cm thickness, 22 cm diameter). Highly aligned electrospun fibers were fabricated onto the PLLA films using a vertical electrospinner [73] and the following electrospinning parameters: 15 min collection time, 15 kV applied voltage, 1500 rpm wheel rotation speed, 4 cm collection distance, 2 mL/h flow rate, and 23 \pm 1% relative humidity. At least three 4% and 12% PLLA solutions were prepared to fabricate films and aligned PLLA fibers in material triplicate for each experiment

All films that would undergo surface characterization (contact angle and zeta potential analysis) and all electrospun fiber scaffolds were dip-coated in a 4% solution of PLLA in chloroform on all four edges to ensure that the polymer scaffold did not lift from the glass coverslip during the biomaterial surface coating process or experiments that followed.

2.5. Biomaterial surface coatings

Surface coatings were investigated to improve mRNA immobilization and subsequent mRNA delivery to cells. PLLA films and electrospun fibers were sterilized under UV for 30 min. Immediately before coating, the films and fibers were plasma-treated with environmental air on the medium setting for 1 min with venting every 10 sec using an Expanded Plasma Cleaner to improve surface hydrophilicity. The coating solution compositions, coating times, and coating procedure for the DSS- and pDOPA-coated groups were based on ongoing work and previous work conducted in the Sing Yan Chew Laboratory [61,65-70], respectively. Briefly, the coating solutions consisted of 1) dextran sulfate sodium salt (DSS) and sodium chloride (NaCl) in sterile 1x PBS or 2) 3,4-dihydroxy-L-phenylalanine (L-DOPA), N,N-Bis(2-hydroxyethyl)glycine (BICINE), and NaCl in sterile deionized water (diH2O) adjusted to pH 8.5 with sodium hydroxide (NaOH). The 15 mm x 15 mm PLLA films or fibers were placed flat in a sterile 12-well plate and submerged in 1.5 mL of the respective coating solution, while the 24 mm x 50 mm PLLA films were placed flat in a 60-mm dish and submerged in 5.5 mL of the respective coating solution. The plate was then placed on a VWR mini orbital shaker (15 mm orbit) at 200 rpm to maintain gentle agitation of the coating solution throughout the coating duration. After coating, each scaffold was washed 3x with sterile diH $_2$ O and dried overnight at 40 $^{\circ}$ C in a vacuum oven. The coating solution compositions and coating times for all DSS- and pDOPA-coated groups investigated are listed in **Table S3**, and coating characterization and reasoning for selecting the optimal DSS- and pDOPA-coated groups are detailed in the supplementary results. **Table 1** summarizes the optimal DSS and pDOPA coating conditions selected to functionalize the PLLA surfaces for further material characterization and *in vitro* testing.

2.6. Biomaterial surface characterization

2.6.1. FTIR

The 15 mm x 15 mm Uncoated PLLA and DSS- and pDOPA-coated electrospun fiber groups were removed from the glass coverslip and analyzed on a NicoletTM iS5 FTIR Spectrometer to investigate the chemical properties of the fiber surface. The mean absorbance spectrum of each group was obtained from \sim 500-4000 cm⁻¹ and normalized to their respective base (minimum) and peak (maximum) values through minimum-maximum normalization. Three separate scaffolds were analyzed per group (n = 3).

2.6.2. Static water contact angle

The static water contact angle on uncoated PLLA and DSS- and pDOPA-coated film groups was measured using a Kruss DSA100 Drop Shape Analyzer to investigate the surface wettability. Contact angle measurements were conducted on 15 mm x 15 mm film samples rather than electrospun fibers, as the water droplet would spread directionally along the fibers introducing a confounding variable. A 3 μ L droplet volume was used, and the angles at the liquid–vapor and solid–liquid interface were fit on the Drop Shape Analysis 4 software. Three droplets were analyzed on each film, averaging each measurement's left and right angles, and three separate films were analyzed per group (n = 3).

2.6.3. Zeta potential

The zeta potential of uncoated PLLA and DSS- and pDOPA-coated film samples was measured by an Anton Paar SurPASSTM 3 Electrokinetic Analyzer for solid surface analysis using an adjustable gap cell to determine the material surface charge. The 24 mm x 50 mm uncoated PLLA and DSS- and pDOPA-coated film groups were removed from the glass and cut to 20 mm x 10 mm to fit into the sample holder. All measurements were performed in a 10 mM KCl solution titrated to a physiologically relevant pH of 7.4 (7.469 \pm 0.178) using the instrument's automated titration system. Each run consisted of five zeta potential measurements; however, only the last three measurements for each run were analyzed to ensure the system was under equilibrium. Three separate runs were performed for each film group (n = 3).

2.7. Electrospun fiber morphological characterization

The morphological features of the uncoated PLLA and 0.5DSS4hand 2pDOPA4h-coated electrospun fiber groups were visually assessed and quantified to ensure consistency among batches and groups, as changes in these features can affect cell response. Uncoated PLLA and 0.5DSS4h- and 2pDOPA4h-coated PLLA fibers were sputter-coated with approximately 1 nm of Au/Pd using a Hummer V Technics sputter coater and then imaged via scanning electron microscopy (SEM) to visualize each fiber group. Images were captured on a versa 3D Dual Beam SEM using an accelerating voltage of 2 kV as described previously [72]. Images for morphological characterization were captured at a 2500x magnification, and representative images were captured at a 1000x magnification.

Table 1Summary table of optimal surface coatings.

Coating name	Coating solution	Coating time
0.5DSS4h	0.5 mg/mL DSS, 1M NaCl, 1x PBS	4 h
2pDOPA4h	2 mg/mL L-DOPA, 10 mM BICINE, 250 mM NaCl, diH2O, pH 8.5	4 h

Fiber alignment, fiber diameter, and percent fiber coverage were characterized via FIJI Software as described previously [72]. The fiber alignment, diameter, and percent coverage of the uncoated PLLA fiber scaffolds were characterized, while the fiber diameters of the 0.5DSS4h- and 2pDOPA4h-coated were characterized. 100 fibers per replicate were analyzed to determine fiber diameter, and six fields of view per replicate were analyzed to determine fiber alignment and percent fiber coverage. At least one electrospun fiber scaffold per replicate and three separate replicates per fiber group were analyzed to characterize fiber alignment, fiber diameter, and percent fiber coverage (n=3).

2.8. Lipoplex immobilization

A total of 3 μg of ΨNT-3mRNA was immobilized per fiber scaffold to the uncoated PLLA and 0.5DSS4h- and 2pDOPA4h-coated fibers to load a dose large enough to remain efficacious over a sustained period. The uncoated PLLA and 0.5DSS4h- and 2pDOPA4hcoated fibers were sterilized via UV for 30 min. A 300 µL solution of Polyplus® mRNA buffer containing 3 μg of ΨNT-3mRNA and 6 µL of JetMESSENGER® was pipetted onto each scaffold and incubated at 37 °C for 30 min. This immobilization incubation period was selected based on the eGFPmRNA immobilization pilot study and immobilization time pilot study detailed in the supplementary methods and results. After the 30 min incubation, the immobilization lipoplex solution was removed, and each scaffold was washed with nuclease-free diH2O. The mRNA immobilized groups will be referred to as PLLA+mRNA, 0.5DSS4h+mRNA, and 2pDOPA4h+mRNA going forward. Immobilization solution containing only mRNA buffer (no added lipoplex) was also incubated with a separate set of uncoated PLLA fibers, and each scaffold was washed with nuclease-free diH2O as described above to serve as the negative control PLLA fiber group.

2.9. Ψ NT-3mRNA loading efficiency and release kinetics

2.9.1. Ψ NT-3mRNA quantification

The Quant-iTTM RiboGreenTM RNA reagent kit was used according to a modified version of the manufacturer's protocol to quantify the amount of mRNA in solution and determine the mRNA loading efficiency and release kinetics. The standard curve was constructed by diluting a ΨNT-3mRNA/JetMESSENGER® lipoplex solution to known mRNA concentrations. Highly negatively charged heparin sodium sulfate was added to the standard and unknown sample solutions at a final concentration of 20 μg/mL [58,70], mixed thoroughly, and incubated for 10 min at room temperature to decomplex the mRNA from the JetMESSENGER®. All decomplexed standard and sample solutions were mixed 1:1 with the Quant-iTTM RiboGreenTM RNA reagent, transferred into a black polystyrene 96-well assay plate, incubated for 5 min, and the concentration of mRNA was determined by measuring fluorescence on a Tecan infinite m200 microplate reader.

2.9.2. Loading efficiency

The amount of unbound Ψ NT-3mRNA was assessed using the Quant-iTTM RiboGreenTM RNA reagent kit as described in Section 2.9.1. to calculate the percent loading efficiency. Briefly, the control and experimental immobilization solutions and wash solutions were collected from the PLLA (negative control),

PLLA+mRNA, 0.5DSS4h+mRNA, and 2pDOPA4h+mRNA fibers. The collected samples were stored at -80 $^{\circ}$ C until quantified via QuantiTTM RiboGreenTM. The percentage of the 3 μ g of Ψ NT-3mRNA initially loaded per scaffold present in the immobilization solution and wash solution was summed and subtracted from 100 to obtain the percent loading efficiency. Different immobilization lipoplex solutions were prepared to immobilize mRNA in each replicate, and six replicates were assessed per fiber group (n = 6).

2.9.3. Release kinetics

The amount of released Ψ NT-3mRNA was assessed using the Quant-iTTM RiboGreenTM RNA reagent kit as described in Section 2.9.1. to assess the mRNA release kinetics. After collecting the immobilization and wash solutions from each fiber group, the PLLA (negative control), PLLA+mRNA, 0.5DSS4h+mRNA, and 2pDOPA4h+mRNA fibers were submerged in 1 mL of nuclease-free 1x Tris-EDTA (TE) buffer. The 1 mL of 1x TE was collected and replaced at the following time points: 4, 8, and 12 h, and 1, 2, 3, 4, 5, 6, 7, 10, 14, 21, and 28 days. The collected samples were stored at -80 °C until quantified via Quant-iTTM RiboGreenTM. The percentage of the experimentally loaded ΨNT -3mRNA (based on the respective percent loading efficiency) present in each release solution was summed over the 28 days to obtain the cumulative percent release of experimentally loaded mRNA. Different immobilization lipoplex solutions were prepared to immobilize mRNA in each replicate, and six replicates were assessed per fiber group (n = 6).

2.10. Schwann cell isolation and culture

We investigated the effects of bolus transfection and the electrospun fiber-mediated mRNA delivery platforms on primary rat Schwann cells, as they are the principal glia of the PNS and vital to the peripheral nerve repair process. The animal procedures outlined were approved by the University of Miami's Institutional animal care and use committee (IACUC). The sciatic nerves from three-day-old Sprague Dawley rats (P3) were isolated, and Schwann cells were obtained and purified to >95% purity before cryopreservation [74-76]. Before experimental culture, the Schwann cells were thawed and cultured for 7 days in 1:10 Poly(Llysine)-coated T75 flasks in a cell culture incubator (5% CO₂ and 37 ^oC) with biweekly changes of Schwann cell media containing Dulbecco's Modified Eagle Medium (DMEM) supplemented with 10% fetal bovine serum, 1% penicillin-streptomycin, 1% GlutaMAXTM, 3 μM forskolin, and 1.25 nM heregulin. Schwann cells expanded to passages three and four were used for all experiments.

2.11. Schwann cell adhesion

Schwann cell adhesion on the uncoated PLLA and 0.5DSS4h-and 2pDOPA4h-coated fibers with and without immobilized Ψ NT-3mRNA/jetMESSENGER® lipoplexes was assessed to determine if the surface coatings or presence of lipoplexes affected cell adhesion. Primary rat Schwann cells were seeded at 100,000 cells per scaffold (\sim 444 cells/mm²) in Schwann cell media onto the following 15 mm x 15 mm electrospun fiber scaffold groups: PLLA (negative control), 0.5DSS4h, 2pDOPA4h, PLLA+mRNA, 0.5DSS4h+mRNA, and 2pDOPA4h+mRNA. The cells were cultured in a cell culture incubator (5% CO2 and 37 °C) for 24 h. After 24 h, Schwann cell cultures were fixed with 4% (v/v) PFA in 1x PBS for 15 min, washed

with 1x PBS three times, blocked with 0.1% (v/v) TritonTM-x 100 and 5% (w/v) BSA in 1x PBS for 1 h, incubated with a 1:1000 dilution of DAPI nuclear stain in 1x PBS for 15 min, and then washed with 1x PBS three times. Three separate replicates were cultured for each fiber group (n = 3).

Images were captured using MetaMorph® Premier 7.7.3.0 imaging software and a 289 Olympus IX-81 confocal microscope at a 20x magnification. FIJI software was used to process and analyze all images identically. The 2D maximum intensity projection of each image was obtained, and the background was subtracted using a rolling ball algorithm with a radius of 50 pixels. The number of cells per image was determined by semi-automatically thresholding each processed DAPI channel image and then using the analyze particles setting on FIJI software. The area of the field of view was determined for a 20x image. These values were used to determine the number of cells per area. Six fields of view were captured and analyzed per coverslip, and three separate coverslips were analyzed per fiber group (n=3).

2.12. Schwann cell protein secretion

Schwann cell NT-3 secretion into culture media was assessed using a rat NT-3 ELISA kit to determine if the electrospun fiber-mediated mRNA delivery platforms induced increased, sustained Schwann cell NT-3 secretion. Schwann cells were seeded at 100.000 cells per scaffold ($\sim 444 \text{ cells/mm}^2$) in Schwann cell media onto the following 15 mm x 15 mm electrospun fiber scaffold groups: PLLA (negative control), PLLA+mRNA, 0.5DSS4h+mRNA, and 2pDOPA4h+mRNA. In addition, Schwann cells cultured onto negative control PLLA fibers and transfected with bolus addition of lipoplex containing 1 µg ΨNT-3mRNA to 2 µL jetMESSEN-GER® or 3 μg ΨNT-3mRNA to 6 μL jetMESSENGER® per sample served as the positive control fiber groups and will be referred to as 1µgBolus+mRNA and 3µgBolus+mRNA going forward. The Schwann cells were cultured in a cell culture incubator (5% CO₂ and 37 °C), and culture media was collected from each sample and replaced at 1, 2, 3, 4, 5, 6, 7, 10, 14, and 21 days after seeding onto mRNA immobilized fibers or after the bolus transfection. The samples were centrifuged at 4 ºC for 10 min at 1500 rcf to remove any debris and aliquoted and stored at -80 °C until analyzed. The amount of rat NT-3 protein was quantified using a rat NT-3 ELISA kit according to the manufacturer's protocol. Different immobilization lipoplex solutions were prepared to immobilize mRNA in each replicate, and four replicates were assessed per fiber group (n = 4).

2.13. Whole DRG isolation and co-culture with Schwann cells

DRG explants were co-cultured in the same media environment as Schwann cells cultured directly onto the electrospun fibermediated mRNA delivery platforms to determine if these platforms induced increased Schwann cell secretion of NT-3 to levels significant enough to improve DRG neurite outgrowth. Coculture media containing a 1:1 ratio of DMEM to neurobasal media (DMEM:NBM) supplemented with 2% fetal bovine serum, 2% B-27®, 1% penicillin-streptomycin, and 250 mM GlutaMAXTM was prepared. Schwann cells were cultured at 100,000 cells per scaffold ($\sim 444 \text{ cells/mm}^2$) in the co-culture media onto the following 15 mm x 15 mm aligned electrospun fiber scaffold groups: PLLA (negative control), PLLA+mRNA, 0.5DSS4h+mRNA, 2pDOPA4h+mRNA, 1µgBolus+mRNA, and 3µgBolus+mRNA. Schwann cells were cultured in these conditions for 24 h in a cell culture incubator (5% CO₂ and 37 °C) before beginning co-culture experiments with whole DRG explants.

The animal procedures outlined were approved by the Rensselaer Polytechnic Institute's IACUC. Whole DRG explants were isolated from P2 Sprague Dawley rats according to previously

described methods [77]. Fig. 1 illustrates the DRG explant and Schwann cell co-culture set-up, which attempts to mimic the signaling environment between Schwann cells and neurons following graft implantation [5,78–80] and enables investigation of the effects of Schwann cell NT-3 secretion on DRG neurite outgrowth. Briefly, in-house 3D printed polylactic acid transwells were placed into each well containing the Schwann cell-seeded fibers. A separate set of negative control PLLA fibers were plasma-treated as described in Section 2.5 to improve DRG adhesion. The PLLA fibers were submerged in the conditioning co-culture media suspended above the Schwann cell-seeded fiber scaffolds by the transwells. Three whole DRG explants were cultured onto each PLLA fiber scaffold suspended in the transwell. The DRG explants were co-cultured with Schwann cells for 4 days in a cell culture incubator (5% CO2 and 37 °C).

2.14. Whole DRG immunocytochemistry and neurite outgrowth analysis

Confocal images of immunocytochemically-labeled DRG were captured and assessed to investigate neurite outgrowth. After the 4-day co-culture, the DRG explants were fixed, washed, and blocked as described in Section 2.11. Next, the DRG were incubated overnight at 4 °C in a primary antibody solution containing 0.1% (v/v) TWEEN®-20 and 5% BSA with a 1:500 dilution of mouse polyclonal RT-97 primary antibody in 1x PBS. The following morning, the DRG were washed with 1x PBS three times and incubated in a secondary antibody solution containing 0.1% TWEEN®-20 and 5% BSA with a 1:1000 dilution of Alexa Fluor donkey antimouse 488 secondary antibody in 1x PBS for 1 h. Finally, the DRG were stained with DAPI nuclear stain and washed as described in Section 2.11.

Images were captured at a 4x magnification and processed as described in Section 2.11. Each processed whole DRG image was stitched using Photoshop CS2. Neurite outgrowth from DRG explants was assessed by quantifying neurite extension and area. The length of the ten longest neurites extending from the body of each DRG explant was measured using the line tool in FIJI software, and the average maximum neurite extension was calculated for each whole DRG explant [81,82]. Next, the whole DRG body was excluded from each image, and the percent area covered by the neurites extending from the DRG explant body was quantified using a semi-automated thresholding FIJI plugin. Each whole DRG was considered an individual replicate, and 24 to 27 whole DRG were analyzed per culture condition (n = 24 - 27).

2.15. Statistical analysis

All statistical analyses were performed using GraphPad Prism 9.3.1. Normality was assessed via a D'Agostino-Pearson Test or a Shapiro-Wilks test if the data set was too small to assess via D'Agostino-Pearson. A One-Way ANOVA with a Tukey's multiple comparisons post hoc test was used for normally distributed data and comparisons against all groups. A One-Way ANOVA with a Dunnett's multiple comparisons post hoc test was used for normally distributed data and comparisons against a single group. Finally, A Kruskal-Wallis with Dunn's multiple comparisons post hoc test was used if the data were not normally distributed.

3. Results

Table 2 summarizes the control and experimental groups investigated in the main text, and all groups mentioned will be designated as the indicated group name in the following sections.

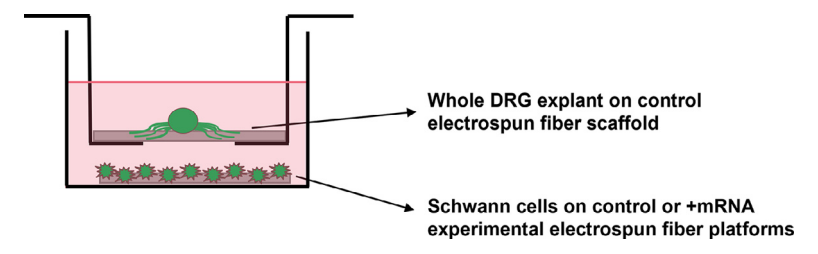


Fig. 1. Schematic of the Schwann cell and whole DRG explant co-culture. Schwann cells are cultured on PLLA (negative control), PLLA+mRNA, 0.5DSS4h+mRNA, 2pDOPA4h+mRNA, 1µgBolus+mRNA, or 3µgBolus+mRNA electrospun fiber platforms that are resting in the bottom of the well. Whole DRG explants are cultured on negative control PLLA electrospun fiber scaffolds submerged in the same media and suspended above the Schwann cell cultures via a polylactic acid transwell.

 Table 2

 Summary table of control and experimental electrospun fiber groups.

Group name	Biomaterial	Coating concentration	Coating time	mRNA delivery
PLLA	Aligned PLLA electrospun fibers	N/A	N/A	N/A
(Negative control)				
0.5DSS4h	Aligned PLLA electrospun fibers	0.5 mg/mL DSS	4 h	N/A
2pDOPA4h	Aligned PLLA electrospun fibers	2 mg/mL L-DOPA	4 h	N/A
PLLA+mRNA	Aligned PLLA electrospun fibers	N/A	N/A	mRNA lipoplexes immobilized to fiber surface
0.5DSS4h+mRNA	Aligned PLLA electrospun fibers	0.5 mg/mL DSS	4 h	mRNA lipoplexes immobilized to fiber surface
2pDOPA4h+mRNA	Aligned PLLA electrospun fibers	2 mg/mL L-DOPA	4 h	mRNA lipoplexes Immobilized to fiber surface
1µgBolus+mRNA (Positive control)	Aligned PLLA electrospun fibers	N/A	N/A	Bolus addition of mRNA lipoplexes carrying 1 µg mRNA per well
3μgBolus+mRNA (Positive control)	Aligned PLLA electrospun fibers	N/A	N/A	Bolus addition of mRNA lipoplexes carrying 3 µg mRNA per well

Table 3 Characterization of approximate Ψ NT-3mRNA lipoplex size, polydispersity, and charge.

Lipoplex	Hydrodynamic Diameter	Polydispersity Index	Zeta Potential
ΨNT3mRNA/JetMESSENGER®	$242.5 \pm 32.6 \text{ nm}$	$15.0\pm4.4\%$	42.1 ± 1.3 mV

3.1. Successful formation of cationic, nanoscale mRNA/JetMESSENGER® lipoplexes for efficient mRNA delivery

Table 3 summarizes the approximate size (hydrodynamic diameter), polydispersity, and surface charge (zeta potential) of the Ψ NT-3mRNA/JetMESSENGER® lipoplexes in suspension. Complexation of the Ψ NT-3mRNA or eGFPmRNA with JetMESSENGER® resulted in a monodisperse population of lipoplexes of similar size and charge (Table S4), illustrated by the overlapping size distribution and zeta potential distribution peaks (Fig. S1). Bolus delivery of eGFPmRNA/JetMESSENGER® lipoplexes revealed JetMESSENGER® effectively delivered eGFPmRNA to Schwann cells with high efficiency, resulting in \geq 95% of cells expressing eGFP over the first 3 days and 18.6 \pm 10.3% of cells still expressing detectable levels of eGFP by day 7 post-transfection (supplementary results and Fig. S2).

3.2. Surface coatings alter PLLA surface wettability and charge

Refer to the supplementary material for images of uncoated and coated PLLA electrospun fibers (Fig. S3), preliminary work for the selection of the optimal DSS and pDOPA coating groups (Fig. S4), and the chemical structures of poly(lactic acid) (PLA), DSS, and pDOPA (Fig. S5). Fig. 2 shows the resulting FTIR spectrum labeled with key identifying peaks and the contact angle and zeta potential data of the optimal 0.5DSS4h- and 2pDOPA4h-coated experimental groups compared to the uncoated PLLA control group. FTIR revealed no noticeable change between the uncoated PLLA adsorption spectrum and the 0.5DSS4h- and 2pDOPA4h-coated fiber spectra (Fig. 2A). The static water contact angles of the 0.5DSS4h (66.4 \pm 2.6°)- and 2pDOPA4h (63.0 \pm 2.2°)-coated film groups were significantly lower than the uncoated PLLA film group (77.8 \pm 1.7°) (Fig. 2B), indicating improved surface hydrophilicity of the coated

groups. Additionally, the zeta potential of the 0.5DSS4h (-66.0 \pm 3.6 mV)- and 2pDOPA4h (-67.2 \pm 3.2 mV)-coated film groups was significantly more negative than the uncoated PLLA film group (-37.4 \pm 5.5 mV) (Fig. 2C), indicating the coated groups possessed a more negative surface charge. Material surface characterization for additional coating groups is provided in the supplementary material (Fig. S5&S6).

3.3. Surface coatings do not alter electrospun fiber scaffold morphology

The SEM images of the uncoated PLLA and 0.5DSS4h- and 2pDOPA4h-coated fiber scaffolds show no visible difference in fiber morphology (Fig. 3A). Further, the mean fiber diameter of the uncoated PLLA fibers (1.98 \pm 0.38 $\mu m)$ was statistically similar to the mean fiber diameter of the 0.5DSS4h (1.99 \pm 0.23 $\mu m)$ - and 2pDOPA4h (1.96 \pm 0.20 $\mu m)$ -coated fiber groups (p> 0.05), indicating that the coatings did not alter fiber diameter (Fig. 3B). The FFT analysis of the uncoated PLLA fiber group displayed high fiber alignment, illustrated by the sharp intensity peak with an area under the curve of 15.79 \pm 4.79 (Fig. 3C). The PLLA fibers were collected at a near-monolayer density with some overlap, resulting in a percent fiber coverage over 100% (113.9 \pm 8.0%) (Fig. 3D).

3.4. Electrospun fiber platforms support immobilization and release of ΨNT -3mRNA

Refer to the supplementary material for preliminary testing of the Ψ NT-3mRNA/JetMESSENGER® lipoplex immobilization time (Fig. S7). The percent loading efficiencies (and resulting mass) of the initial 3 µg (3000 ng) of Ψ NT-3mRNA loaded per scaffold were similar amongst groups, resulting in 72.7 \pm 4.8% (2180 \pm 145 ng) for PLLA+mRNA fibers, 72.2 \pm 1.0 % (2165 \pm 29 ng)

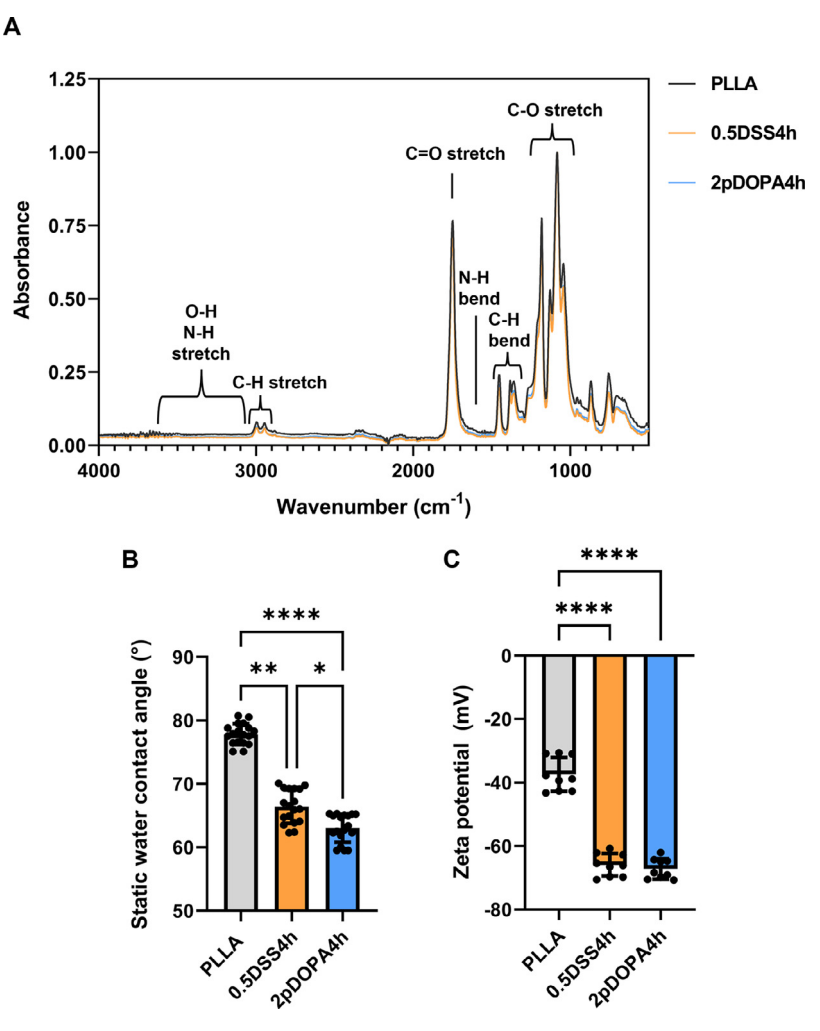


Fig. 2. The 0.5DSS4h and 2pDOPA4h surface coatings altered PLLA wettability and charge. A) FTIR minimum-maximum normalized adsorption spectra for uncoated PLLA fibers (black), 0.5DSS4h-coated PLLA fibers (orange), and 2pDOPA4h-coated PLLA fibers (blue) labeled with key identifying peaks. B) The static water contact angle on uncoated PLLA films (grey), 0.5DSS4h-coated films (orange), and 2pDOPA4h-coated films (blue) represented by the mean (9) \pm the standard deviation and overlayed with the individual data points. Statistical significance compared to each group was assessed using a Kruskal-Wallis test and Dunn's multiple comparisons *post hoc* test (n = 3). C) The zeta potential of uncoated PLLA films (grey), 0.5DSS4h-coated films (orange), and 2pDOPA4h-coated films (blue) represented by the mean (mV) \pm the standard deviation and overlayed with the individual data points. Statistical significance compared to each group was assessed using a one-way ANOVA and Tukey's multiple comparisons *post hoc* test (n = 3). *p < 0.05; **p < 0.05; **p < 0.001; *****p < 0.0001.

for 0.5DSS4h+mRNA fibers, and 76.2 \pm 2.5% (2286 \pm 75 ng) for 2pDOPA4h+mRNA fibers (Fig. 4A). The 0.5DSS4h- and 2pDOPA4h-coated fibers groups exhibited an increased rate of Ψ NT-3mRNA release, particularly over the first 7 days, compared to the uncoated PLLA fiber group (Fig. 4B). Based on the Ψ NT-3mRNA loading efficiency determined for the respective samples and replicates, the cumulative percent (and mass) of experimentally loaded Ψ NT-3mRNA released over 28 days from the PLLA+mRNA, 0.5DSS4h+mRNA, and 2pDOPA4h+mRNA fiber groups were 20.0 \pm 1.7% (435 \pm 42 ng), 30.4 \pm 3.2% (658 \pm 65 ng), and 31.7 \pm 10.0% (726 \pm 236 ng), respectively (Fig. 4B). No detectable mRNA was observed from the negative control PLLA immobilization solution, wash solution, or release solutions (Fig. S8).

3.5. Electrospun fiber platforms support Schwann cell adhesion

Fig. 5A shows confocal images used to determine the number of adherent Schwann cells per mm² after 24 h. Schwann cell adhesion onto the uncoated PLLA (589 \pm 72 cells/mm²) fibers was similar to the 0.5DSS4h (541 \pm 94 cells/mm²)- and 2pDOPA4h (590 \pm 96 cells/mm²)-coated fiber groups (p>0.05), indicating the 0.5DSS4h and 2pDOPA4h coatings alone do not affect Schwann

cell adhesion compared to the uncoated PLLA fibers. Similarly, Schwann cell adhesion to the PLLA+mRNA (594 \pm 135 cells/mm²) and 0.5DSS4h+mRNA (540 \pm 78 cells/mm²) fiber groups was similar to that observed in the non-mRNA immobilized fiber groups, indicating that the presence of mRNA on these fiber groups did not affect Schwann cell adhesion. Conversely, Schwann cell adhesion decreased in the 2pDOPA4h+mRNA fiber group (498 \pm 79 cells/mm²) compared to the uncoated PLLA and 2pDOPA4h-coated fiber groups (Fig. 5B), indicating the mRNA lipoplex presence on 2pDOPA4h+mRNA fiber group influences Schwann cell adhesion.

3.6. Electrospun fiber-mediated delivery of $$\Psi NT\text{-}3mRNA/JetMESSENGER}$ lipoplexes increases Schwann cell secretion of NT-3 protein$

Fig. 6 and Fig. S9 show the differences in Schwann cell secretion of NT-3 protein into culture media over 21 days, and Table S5 lists the mean amount of NT-3 protein secreted \pm the standard deviation at each time point. Schwann cells cultured on the 2pDOPA4h+mRNA fibers secreted increased amounts of NT-3 protein 1, 2, 3, 4, 5, 6, 7, 14, and 21 days post-seeding compared to those cultured on the negative control PLLA fibers (Fig. 6).

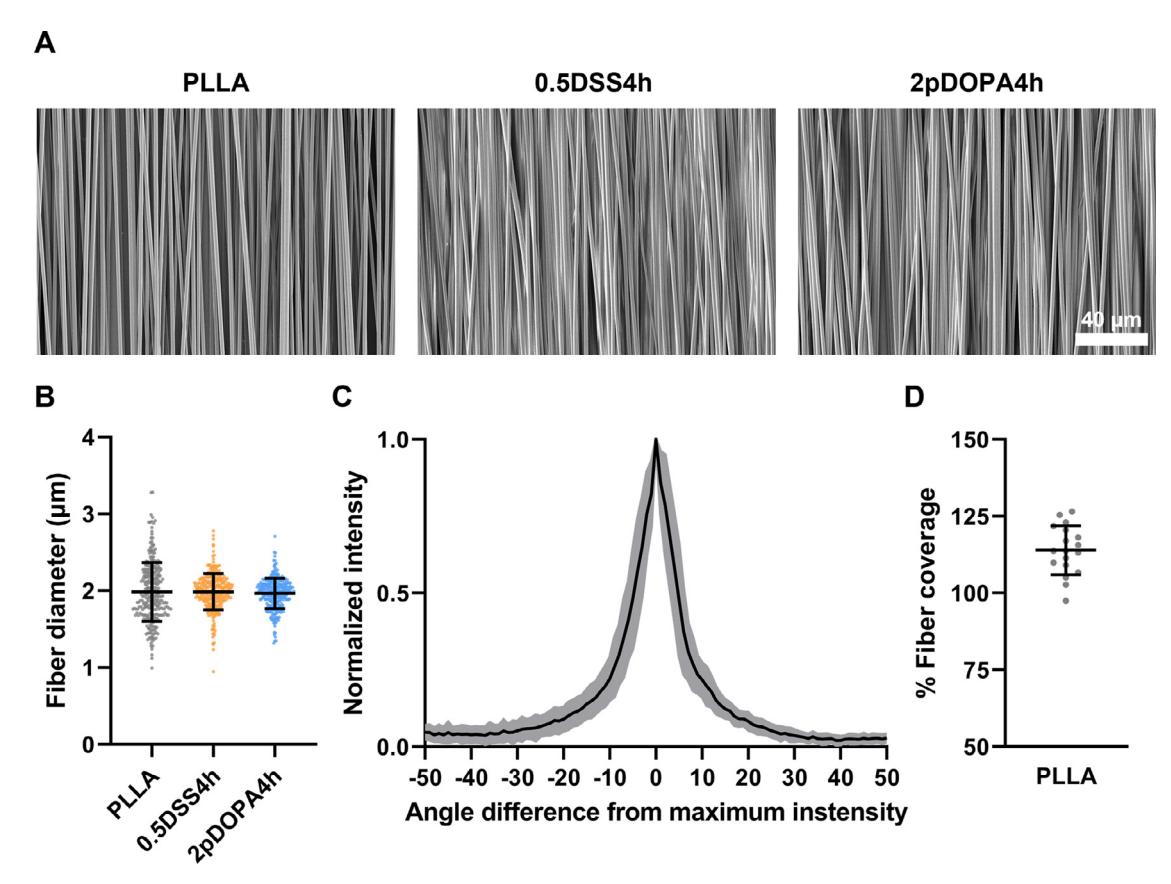


Fig. 3. The 0.5DSS4h and 2pDOPA4h surface coatings did not alter PLLA fiber morphology. A) SEM images of uncoated PLLA fibers, 0.5DSS4h-coated fibers, and 2pDOPA4h-coated fibers (captured at 1000x magnification, scale bar = 40 μ m). B) The fiber diameter of uncoated PLLA fibers (grey), 0.5DSS4h-coated fibers (orange), and 2pDOPA4h-coated fibers (blue) represented by the mean (μ m) \pm the standard deviation and underlaid with the individual data points (n = 3). C) Uncoated PLLA fiber alignment was determined using FFT to calculate the minimum-maximum normalized intensity curve represented by the mean (intensity) \pm standard deviation (grey shading). The mean area under the curve (15.79 \pm 4.79 arbitrary units) was determined using the trapezoidal rule (n = 3). D) The percent fiber coverage data of uncoated PLLA fibers (grey) are represented by the mean (\pm) \pm the standard deviation and underlaid with the individual data points (n = 3).

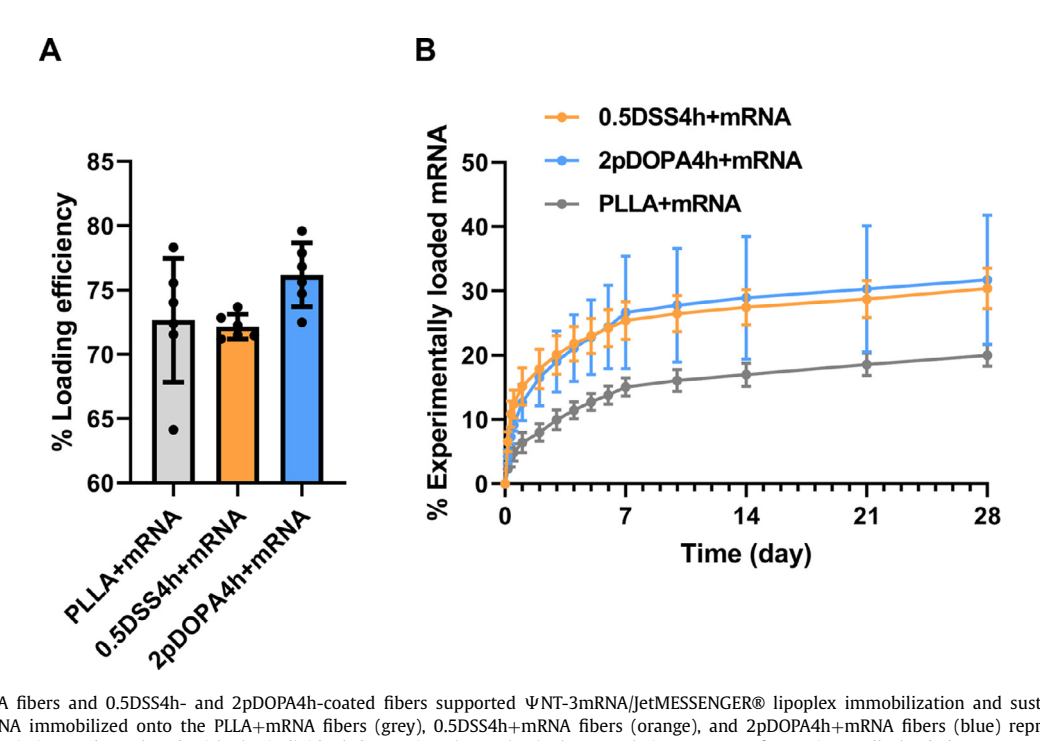


Fig. 4. Uncoated PLLA fibers and 0.5DSS4h- and 2pDOPA4h-coated fibers supported Ψ NT-3mRNA/JetMESSENGER® lipoplex immobilization and sustained release. A) The percent of Ψ NT-3mRNA immobilized onto the PLLA+mRNA fibers (grey), 0.5DSS4h+mRNA fibers (orange), and 2pDOPA4h+mRNA fibers (blue) represented by the mean (%) \pm the standard deviation and overlayed with the individual data points (n = 6). B) The cumulative percent of experimentally loaded Ψ NT-3mRNA released from the PLLA+mRNA fibers (grey), 0.5DSS4h+mRNA fibers (orange), and 2pDOPA4h+mRNA fibers (blue) over 28 days represented by the mean (%) \pm the standard deviation (n = 6).

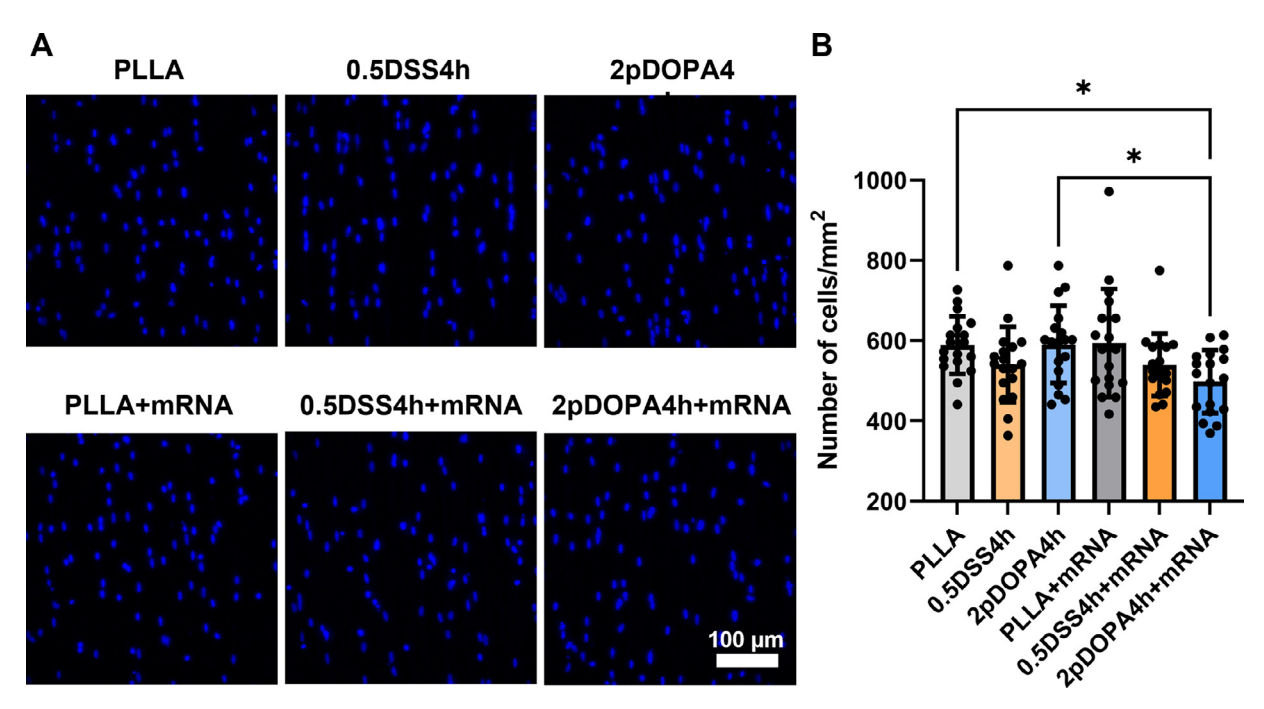


Fig. 5. The uncoated, coated, and Ψ NT-3mRNA/JetMESSENGER® lipoplex-immobilized uncoated and coated PLLA fibers supported Schwann cell adhesion. A) Confocal images of primary rat Schwann cells stained with DAPI (blue) to visualize the nuclei following 1 day in culture on each fiber group (captured at 20x magnification; scale bar = 100 μm). B) The number of Schwann cells per area on the uncoated PLLA fibers (light grey), 0.5DSS4h-coated fibers (light orange), 2pDOPA4h-coated fibers (light blue), PLLA+mRNA fibers (grey), 0.5DSS4h+mRNA fibers (orange), and 2pDOPA4h+mRNA fibers (blue) represented by the mean (cells/mm²) \pm the standard deviation and overlayed with the individual data points. Statistical significance compared to each group was assessed using a Kruskal-Wallis test and Dunn's multiple comparisons post hoc test (n = 3). *p < 0.05.

Schwann cells cultured on the 2pDOPA4h+mRNA fibers also secreted increased amounts of NT-3 protein 1, 2, and 21 days post-seeding compared to those cultured on the PLLA+mRNA fibers; 1, 2, 6, and 21 days post-seeding compared to those cultured on the 1µgBolus+mRNA positive control fiber group; and 21 days post-seeding compared to those cultured on the 0.5DSS4h+mRNA fibers or 3µgBolus+mRNA positive control fiber group (Fig. 6). Additionally, the Schwann cells cultured on the 0.5DSS4h+mRNA fibers secreted increased amounts of NT-3 protein 4 and 5 days post-seeding than those cultured on the negative control PLLA fibers (Fig. 6). Although the trends in Schwann cell NT-3 protein secretion remained similar, no significant differences were observed amongst the groups at the 10-day time point (Fig. S9).

3.7. Electrospun fiber-mediated delivery of $$\Psi NT\text{-}3mRNA/JetMESSENGER}$ lipoplexes increases whole DRG neurite outgrowth$

Fig. 7A and Fig. S10A show DRG images captured via confocal microscopy. The resulting neurite extension and neurite area trends were similar (Fig. 7B&C and Fig. S10B&C). The DRG cultured in the presence of Schwann cells cultured on the 2pDOPA4h+mRNA fibers extended longer neurites (2.66 \pm 0.62 mm) than those in the presence of Schwann cells on the negative control PLLA fibers (1.84 ± 0.40 mm), PLLA+mRNA fibers (1.94 \pm 0.49 mm), or 0.5DSS4h+mRNA fibers (2.27 \pm 0.44 mm) (Fig. 7B). The DRG cultured in the presence of Schwann cells on the 0.5DSS4h+mRNA fibers also extended longer neurites than those in the presence of Schwann cells cultured on the negative control PLLA fibers (Fig. 7B). The DRG cultured in the presence of Schwann cells on the 2pDOPA4h+mRNA fibers extended neurites that covered a larger area (1.02 \pm 0.37 mm²) than those in the presence of Schwann cells cultured on the negative control PLLA (0.62 \pm 0.26 mm²) or PLLA+mRNA (0.62 \pm 0.32 mm²) (Fig. 7C).

Additionally, in previous work conducted in the Gilbert Laboratory, D'Amato et al. reported that whole DRG cultured without additional Schwann cells on aligned, smooth PLLA fibers extended neurites with an average length of 1.77 \pm 0.17 mm and area of 0.67 \pm 0.10 mm² [77]. These values agree well with the neurite extension and area data obtained in this study from DRG cultured in the presence of Schwann cells cultured on negative control PLLA fibers. This indicates that mRNA delivery and increased Schwann cell secretion of NT-3 likely had a greater impact on DRG neurite outgrowth compared to the presence of additional Schwann cells alone.

4. Discussion

In this study, we developed the first electrospun fiber-mediated mRNA delivery platform for neural regeneration applications and investigated the platform's efficacy with primary PNS cells *in vitro*. The major findings of this study are 1) the PLLA+mRNA, 0.5DSS4h+mRNA, and 2pDOPA4h+mRNA aligned electrospun fiber platforms sustained detectable release of Ψ NT-3mRNA for at least 28 days, 2) the 2pDOPA4h+mRNA aligned electrospun fibers increased primary rat Schwann cell secretion of NT-3 for at least 21 days, and 3) DRG cultured on uncoated PLLA aligned electrospun fibers in the presence of Schwann cells cultured directly on 2pDOPA4h+mRNA aligned electrospun fibers extended the longest neurites and covered the largest area along the PLLA electrospun fibers. These findings revealed that the 2pDOPA4h+mRNA electrospun fiber platform was optimal in inducing Schwann cell secretion of bioactive NT-3 capable of stimulating DRG neurite outgrowth.

Investigation into mRNA therapeutics is growing rapidly and can potentially overcome limitations of protein and DNA therapeutics, such as short half-life and insertional mutagenesis [83,84]. Still, the instability and immunogenicity of mRNA and the challenge of delivering an efficacious dose to a target location slow the

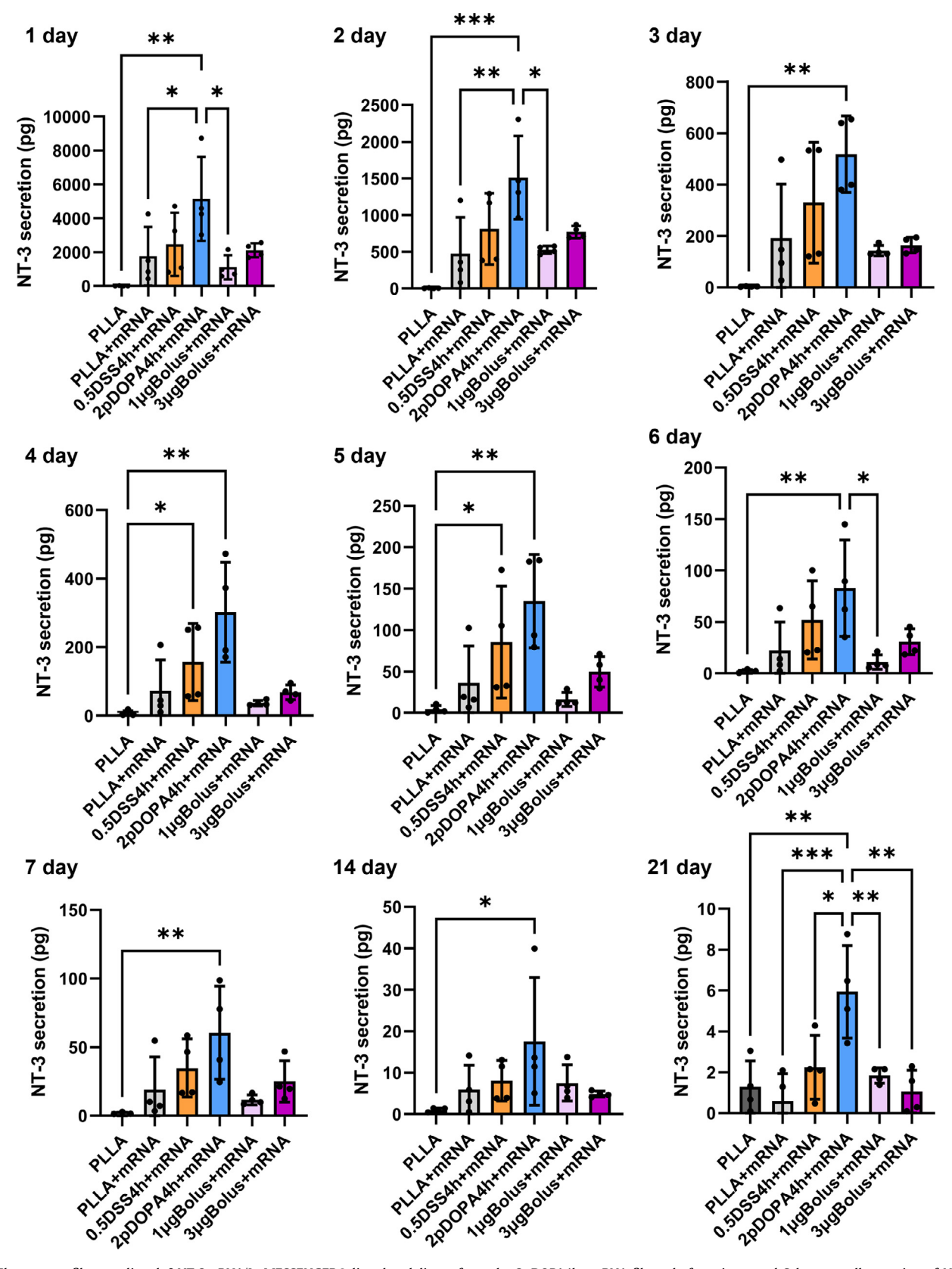


Fig. 6. Electrospun fiber-mediated ΨNT-3mRNA/JetMESSENGER® lipoplex delivery from the 2pDOPA4h+mRNA fiber platform increased Schwann cell secretion of NT-3 protein over 21 days. Quantification of the amount of NT-3 protein present in the Schwann cell media 1, 2, 3, 4, 5, 6, 7, 14, and 21 days following culture onto the PLLA negative control fibers (dark grey), PLLA+mRNA fibers (grey), 0.5DSS4h+mRNA fibers (orange), 2pDOPA4h+mRNA fibers (blue), 1 μ gBolus+mRNA positive control fibers (pink), and 3 μ gBolus+mRNA positive control fibers (purple) represented by the mean (pg) \pm standard deviation and overlayed with the individual data points. Statistical significance compared to each group at the respective time point was assessed using a one-way ANOVA and Tukey's multiple comparisons *post hoc* test (1, 2, 6, 14, 21 days) or a Kruskal-Wallis test and Dunn's multiple comparisons *post hoc* test (3, 4, 5, 7 days) (n = 4). *p < 0.05; **p < 0.05; **p < 0.001.

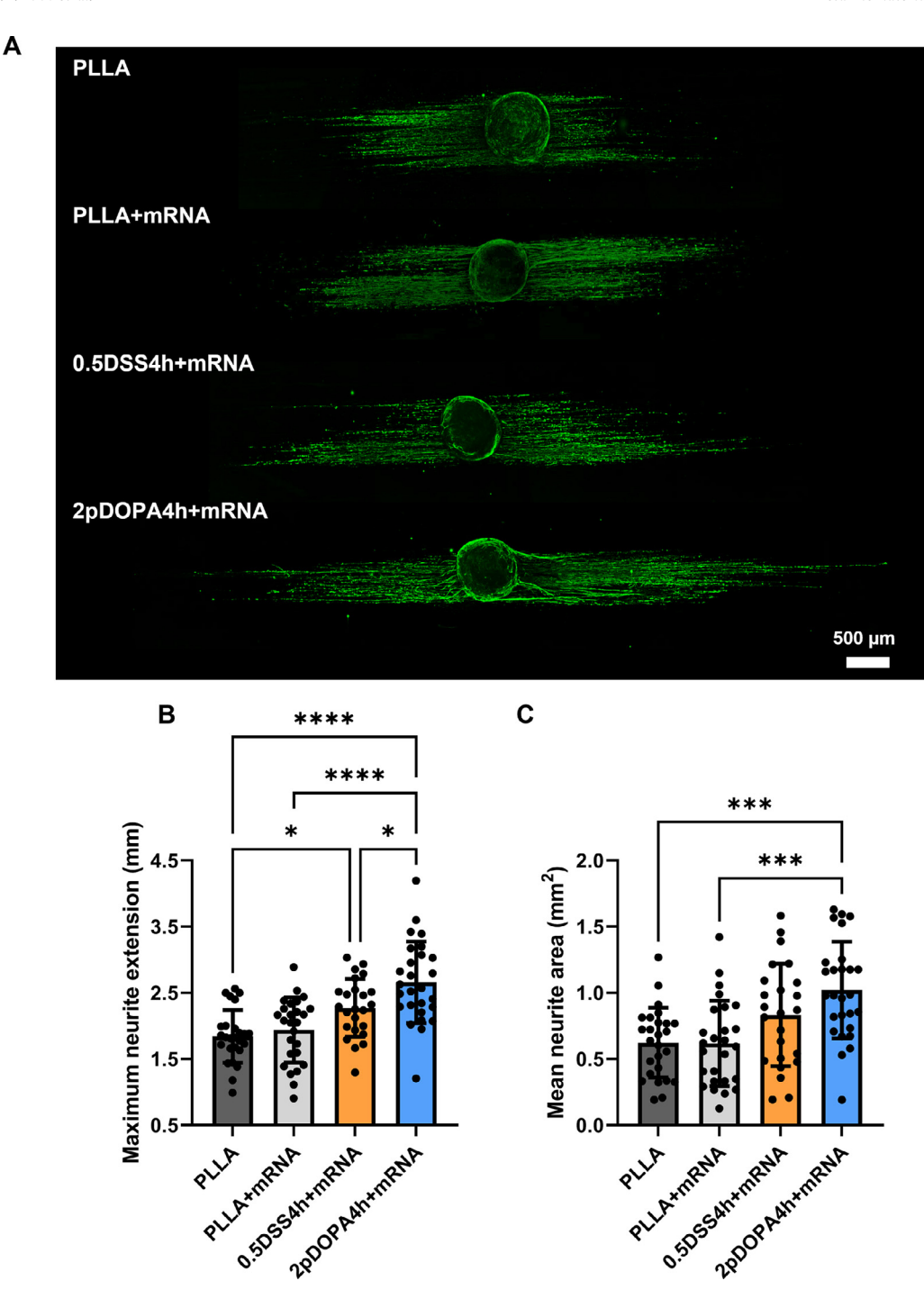


Fig. 7. The 2pDOPA4h+mRNA aligned electrospun fiber platforms enabled Schwann cells to better support neurite outgrowth from whole DRG. A) Confocal images of primary rat whole DRG explants stained against RT97 (green) to visualize the neurites following 4 days in culture on negative control PLLA aligned electrospun fibers in the presence of primary rat Schwann cells cultured directly on negative control PLLA, PLLA+mRNA, 0.5DSS4h+mRNA, and 2pDOPA4h+mRNA aligned electrospun fiber platforms (captured at 4x magnification; scale bar = 500 μ m). B) Neurite extension data following culture in the presence of the negative control PLLA (dark grey), PLLA+mRNA (grey), 0.5DSS4h+mRNA (orange), and 2pDOPA4h+mRNA (blue) fiber platforms are represented by the mean length of the ten longest neurites extending outward from the DRG body (mm) \pm standard deviation and overlayed with the individual data points. Statistical significance compared to each group was assessed using a one-way ANOVA (grey) 0.5DSS4h+mRNA (orange), and 2pDOPA4h+mRNA (blue) fiber platforms are represented by the mean area that the neurites covered (mm²) \pm standard deviation and overlayed with the individual data points. Statistical significance compared to each group was assessed using a one-way ANOVA and Tukey's multiple comparisons post hoc test (n = 24-27). ** *p < 0.00; *** *p < 0.001; **** *p < 0.0001.

development of mRNA therapeutics for tissue engineering and regenerative medicine [50,85,86]. In this study, we utilized an ARCA cap and the modified nucleotide pseudouridine-5'-triphosphate (Ψ) , known to improve synthetic mRNA stability and subsequent translation into the desired protein without inducing a severe

immune response [48,51–56,87]. Additionally, cationic gene delivery vehicles, like JetMESSENGER®, have been shown to improve cellular uptake and protect mRNA against immune system detection and nucleolytic degradation [51,53,54,88–90]. Effective cationic transfection agents typically condense the anionic genetic

cargo into nanoparticles with a hydrodynamic size ranging from $\sim 50\text{-}200$ nm while imparting a slight positive charge onto the particle [91]. Here, we show that JetMESSENGER® enabled the formation of a monodisperse suspension of cationic mRNA lipoplexes that possessed a similar size and charge observed in previous literature [87] (Table 3) and transfected Schwann cells with high efficiency (**Fig. S2**).

Electrospun fibers have been used to locally deliver therapeutic DNA and RNA interference molecules while providing structural guidance cues [11,12,58-61], but a fibrous platform has yet to be developed to deliver therapeutic mRNA for neural repair applications. To investigate and optimize fibers for immobilization and delivery of cationic mRNA lipoplexes, we immobilized mRNA lipoplexes to either uncoated aligned PLLA fibers or aligned PLLA fibers coated with the anionic substrates pDOPA or DSS. Although PLLA possesses a negative zeta potential under physiological pH, this is likely due to the preferential adsorption of hydroxide anions at the interface of the aqueous liquid and hydrophobic material surface, as PLLA does not possess any reactive, anionic functional groups [92,93]. L-DOPA is a well-characterized mussel-inspired bio-adhesive molecule that is polymerized to form pDOPA onto various surfaces under alkaline conditions, resulting in an abundance of anionic carboxyl groups on the material surface [94,95]. Several studies have coated electrospun fibers with pDOPA to improve immobilization and sustain delivery of cationic complexes carrying non-coding RNA in the form of siRNA, miRNA, or single guide RNA (sgRNA) [12,61,65-70]. For example, Low et al. observed improved gene silencing by immobilizing siRNA/TKO complexes to pDOPA-coated electrospun fibers compared to uncoated electrospun fibers [65], Zhang et al. observed improved gene silencing when immobilizing miRNA/TKO complexes to pDOPA-coated electrospun fibers compared to bolus delivery of miRNA/TKO [61], and Chin et al. observed improved editing efficiencies when immobilizing Cas9:sgRNA/lipofectamine complexes to pDOPA + laminincoated electrospun fibers compared to uncoated electrospun fibers [70]. However, pDOPA-coated electrospun fibers have yet to be investigated with mRNA. Immobilization of the cationic gene delivery vehicles to the pDOPA-coated fibers may occur through electrostatic interactions, hydrophobic interactions, hydrogen bonding, or Shiff base or Michael addition reactions between the o-quinones of pDOPA and amine or thiol functional groups within the gene delivery vehicle [65,96-98]. DSS was investigated as an alternative anionic coating. DSS is a biocompatible polysaccharide that possesses anionic sulfonate groups and was previously employed to immobilize a cationic enzyme to electrospun fibers via electrostatic interactions [71]. However, DSS has not been used to facilitate the immobilization of cationic gene delivery vehicles to electrospun fibers. The chemical structure of JetMESSENGER® is proprietary, so the specific physical and chemical mechanisms that enable immobilization of the cationic mRNA lipoplexes to both substrates in this study are unknown.

We found that the 0.5DSS4h- and 2pDOPA4h-coated substrates exhibited increased surface wettability and anionic characteristics compared to the uncoated PLLA fibers (Fig. 2) while maintaining a high degree of alignment and a fiber diameter of \sim 2 μm (Fig. 3), which are known to be optimal morphological features for fiber-mediated neural regeneration [62,63,82,99–101]. Still, 0.5DSS4h- and 2pDOPA4h-coated substrates showed a similar Ψ NT-3mRNA loading efficiency and appeared to release Ψ NT-3mRNA at an increased rate over the first week compared to the uncoated PLLA fibers (Fig. 4). This observation may, in part, be due to the increased hydrophobicity of the uncoated PLLA fiber group (Fig. 2A) supporting increased nonspecific adsorption of the cationic mRNA lipoplexes compared to the 0.5DSS4h- and 2pDOPA4h-coated fibers. Hydrophobic surfaces facilitate increased nonspecific adsorption from an aqueous solution driven by favor-

able interfacial energetics, which can be irreversible or less reversible than the specific physical or chemical interactions that we hypothesize occur between the cationic mRNA lipoplexes and the 0.5DSS4h- and 2pDOPA4h-coated fibers [102,103].

Materials functionalized with L-DOPA or sulfonate groups like those in DSS can facilitate cell adhesion [104-107]. However, we showed that the 0.5DSS4h and 2pDOPA4h coatings alone did not alter Schwann cell adhesion compared to the uncoated PLLA fibers (Fig. 5). This may be due to the high surface area and ECM mimicking nature of aligned electrospun fibers, known to improve Schwann cell adhesion [100,108-110], overcoming adhesive effects of DSS or pDOPA. We found that the 2pDOPA4h+mRNA fiber platform was the only group to support reduced Schwann cell adhesion after 24 h (Fig. 5). However, the ELISA data showed that the 2pDOPA4h+mRNA fiber platform supported the highest levels of Schwann cell secretion of NT-3 protein after 24 h (Fig. 6), indicating that this fiber platform likely facilitated increased Schwann cell uptake of the Ψ NT-3mRNA/JetMESSENGER® lipoplexes. Uptake of cationic molecules is known to induce cellular toxicity [90,111-113]; thus, the increased uptake of cationic mRNA lipoplexes by Schwann cells on the 2pDOPA4h+mRNA fiber platform may explain why we observed decreased adhesion and increased NT-3 secretion after 24 h on this platform.

We found that the 2pDOPA4h+mRNA fiber platform supported the highest Schwann cell secretion of NT-3 protein over 21 days (Fig. 6). Gene delivery from electrospun fibers can be facilitated through the release of the genetic material and uptake by cells local to the material [58,69] or through direct uptake at the material/cell interface by cells that populate the scaffold [66,70]. Therefore, the ΨNT -3mRNA release from the 2pDOPA4h+mRNA fibers (Fig. 4B) could have, in part, improved mRNA delivery to Schwann cells, resulting in increased NT-3 secretion. Additionally, the 2pDOPA4h surface coating may influence electrospun fiber mechanical properties and surface chemistry in a manner that stimulates direct cellular uptake of the lipoplexes immobilized to the fiber surface, improving transfection efficiency and increasing NT-3 secretion [114-116]. The greatest levels of NT-3 secretion were observed from all experimental groups on day 1 and continued to decrease thereafter. This may, in part, be due to the increased release of Ψ NT-3mRNA at earlier time points and an increased concentration of Ψ NT-3mRNA lipoplexes available on the fiber surface for direct uptake by Schwann cells cultured onto the Ψ NT-3mRNA-loaded electrospun fibers. Whereas, at later time points, ΨNT-3mRNA delivery relied more on direct cellular uptake of the remaining ΨNT-3mRNA lipoplexes immobilized to the fiber surface. Due to the possible combination of mRNA delivery through release from the fiber scaffold and direct uptake from cells cultured onto the fiber surface, it would be beneficial to investigate implantation of this guidance conduit alone or pre-seeded with Schwann cells to determine which method would be most bene-

We found that the DRG neurite outgrowth data reflected those observed in the Schwann cell NT-3 secretion ELISA data. Furthermore, the whole DRG explants cultured in the presence of Schwann cells cultured on the 2pDOPA4h+mRNA fiber platforms extended the longest neurites that covered the greatest area (Fig. 7). In previous literature, NT-3 protein has been added to pure or co-cultured Schwann cells and neurons at concentrations ranging from 10-10⁶ pg/mL to elicit a response on Schwann cells and/or sensory neurons *in vitro* [17,27,29,31,117–119]. Specifically, Santos et al. found NT-3 protein concentrations as low as 5000 pg/mL increased neurite outgrowth from rat DRG explants compared to the unstimulated control [27]. We showed the 2pDOPA4h+mRNA fiber platforms stimulated Schwann cell secretion of NT-3 at a concentration of ~5000 pg/mL at the 1-day time when DRG explant culture began, and the NT-3 concentration at each subsequent time

point fell between 10-10⁶ pg/mL for at least 14 days (Fig. 6 and **Table S5**). These findings indicate that the 2pDOPA4h+mRNA fibers support Schwann cell secretion of NT-3 at levels capable of stimulating DRG neurite outgrowth.

Direct treatment with NT-3 protein supports PNS and central nervous system regeneration, but clinical translation is limited by the protein's short half-life (1.28 \pm 0.07 min) and the need for repeated administration [36,40]. As an alternative, Ad and AAV viral vectors have been used to upregulate the production of NT-3 over a sustained period to increase neurite outgrowth in vitro [28] and improve peripheral nerve regeneration in vivo [36,120-123]. However, Ad and AAV therapeutics are limited by packaging capacity and long-term safety concerns related to immunogenicity or insertional mutagenesis [49,124,125]. mRNA therapeutics provide a nonviral approach to enable transient expression with high efficiency in hard-to-transfect primary PNS cells. To our knowledge, only one prior study investigates NT-3mRNA delivery from biomaterials to improve outcomes following peripheral nerve injury; Yang and colleagues loaded adipose-derived exosomes carrying mRNA transcripts encoding NT-3 into the intraluminal alginate filler of a hollow silicon nerve graft. NT-3mRNA/exosome delivery from the graft increased in vivo levels of NT-3 protein and improved functional outcomes following implantation into a 1 cm rat sciatic nerve injury model compared to unloaded control grafts. Still, regenerative outcomes were inferior to the autograft positive control [126]. This NT-3mRNA/exosome-loaded synthetic nerve graft did not present substantial guidance cues; thus, the regenerative capacity of this synthetic nerve graft could potentially be improved by incorporating aligned electrospun fibers, like those used in this study.

Immobilization of ΨNT-3mRNA/JetMESSENGER® lipoplexes to the 2pDOPA4h fibers enabled the delivery of ΨNT-3mRNA, increased Schwann cell secretion of NT-3, and stimulated DRG neurite outgrowth. However, this platform has several limitations that should be addressed before conducting in vivo studies. First, although the JetMESSENGER® provides some protection for the mRNA, surface immobilization of mRNA lipoplexes directly exposes them to environmental changes, like pH and temperature, that can reduce the bioactivity of highly sensitive mRNA. Second, the current platform does not allow for fine control of the duration and dose of Ψ NT-3mRNA that is delivered. Although the current approach enabled mRNA release for 28 days and increased Schwann cell secretion of NT-3 for 21 days, this will likely need to be extended to enable robust regeneration following traumatic injuries. Lastly, considerable variability in Schwann cell secretion of NT-3 amongst the replicates of each group was observed. This is likely due to biological variability and the variability in the surface coating and immobilization procedures. This considerable variability along with the decrease of NT-3 secretion from Schwann cells cultured on the 2pDOPA4h+mRNA fibers at later time points may, in part, explain why the 2pDOPA4h+mRNA fiber group significantly increased Schwann cell secretion of NT-3 compared to the negative control PLLA fibers at each time point except

The limitations can be overcome by utilizing other mRNA lipoplex loading methods that provide better protection and enable more controlled delivery of the Ψ NT-3mRNA. An alternative method is to incorporate the mRNA lipoplexes within a fiber surface coating. For example, Zhang et al. utilized a layer-by-layer coating technique to immobilize pDNA/PEIpro within the surface coating on aligned electrospun fibers [127]. Another method is to incorporate the mRNA lipoplexes into the core of coaxial electrospun fibers. Coaxial electrospun fibers have been employed in various tissue engineering applications to extend and control the delivery of pDNA [128–131] and RNA interference molecules [132–137]. Still, these methods have yet to be investigated for the delivery of mRNA from electrospun fibers.

The electrospun fiber scaffolds investigated serve as versatile non-viral mRNA delivery platforms. The mRNA transcript, gene delivery vehicle, and surface coatings can be modified to regulate different desired proteins, optimize transfection efficiency, enable targeted delivery, and tune loading efficiency and release kinetics. Additionally, the electrospun fiber morphological characteristics can be tuned to optimize the scaffolds for regeneration of different tissues [12]. Fine-tuning each of these aspects of the electrospun fiber-mediated mRNA delivery platforms enables further optimization for potential use in various tissue engineering applications.

5. Conclusion

In conclusion, we developed the first electrospun fiber-based mRNA delivery platform for neural tissue engineering applications. This versatile platform has the potential to provide cells with tunable topographical features and local, sustained, non-viral delivery of mRNA to guide regenerating tissue and enable transient expression of the desired protein. Here, we fabricated aligned electrospun fibers functionalized with DSS or pDOPA, immobilized cationic ΨNT-3mRNA/JetMESSENGER® lipoplexes to the fiber surface, and characterized their ability to upregulate Schwann cell secretion of NT-3 and, in turn, enhance neurite outgrowth from whole DRG explants in vitro. We found that 2pDOPA4h+mRNA fibers promoted the highest levels of NT-3 protein secretion from Schwann cells over 21 days, which stimulated increased neurite outgrowth from DRG explants compared to the uncoated PLLA control and PLLA+mRNA fiber groups. These observations demonstrate the regenerative potential of the ΨNT-3mRNA/JetMESSENGER® lipopleximmobilized pDOPA-coated aligned electrospun fiber platform and support future testing in an in vivo peripheral nerve injury model.

Declaration of Competing Interest

The authors declare that they have no known competing financial interests or personal relationships that could have appeared to influence the work reported in this paper.

Acknowledgments

We thank Henry L. Puhl III for his advice and feedback regarding the molecular biology techniques used in this study, Derek W. Nelson for constructing the 3D-printed transwell inserts used for co-culture experiments, and Anthony R. D'Amato for his advice and feedback regarding the initial design of the study.

Funding for this work was provided by National Institutes of Health (NIH) R01 Grant (#NS092754) and the New York State Spinal Cord Injury Research Board (NYSCIRB) Institutional Support Grant (#C32245GG) awarded to R.J.G.; National Science Foundation Career Grant (#2045510) awarded to R.H.Z; National Science Foundation Graduate Research Fellowships (#DGE-1744655) awarded to D.L.P. and J.L.F. Any opinions, findings, and conclusions or recommendations expressed in this material are those of the author(s) and do not necessarily reflect the views of the National Science Foundation.

Supplementary materials

Supplementary material associated with this article can be found, in the online version, at doi:10.1016/j.actbio.2022.11.025.

References

[1] , National Institute of Neurological Disorders and Stroke. (2021). https://www.ninds.nih.gov/Disorders/Patient-Caregiver-Education/Fact-Sheets/Peripheral-Neuropathy-Fact-Sheet (accessed February 11, 2022).

- [2] D. Grinsell, C.P. Keating, Peripheral nerve reconstruction after injury: a review of clinical and experimental therapies, Biomed. Res. Int. 2014 (2014) 698256, doi:10.1155/2014/698256.
- [3] S.S. Sunderland, The anatomy and physiology of nerve injury, Muscle Nerve 13 (1990) 771–784, doi:10.1002/mus.880130903.
- [4] R. Deumens, A. Bozkurt, M.F. Meek, M.A.E. Marcus, E.A.J. Joosten, J. Weis, G.A. Brook, Repairing injured peripheral nerves: bridging the gap, Prog. Neurobiol. 92 (2010) 245–276, doi:10.1016/j.pneurobio.2010.10.002.
- [5] S. Houshyar, A. Bhattacharyya, R. Shanks, Peripheral nerve conduit: materials and structures, ACS Chem. Neurosci. 10 (2019) 3349–3365, doi:10.1021/acschemneuro.9b00203.
- [6] J.A. Fishman, M.A. Greenwald, P.A. Grossi, Transmission of infection with human allografts: essential considerations in donor screening, Clin. Infect. Dis. 55 (2012) 720–727, doi:10.1093/cid/cis519.
- [7] B. Safa, J.T. Shores, J.V. Ingari, R.V. Weber, M. Cho, J. Zoldos, T.R. Niacaras, L.J. Nesti, W.P. Thayer, G.M. Buncke, Recovery of motor function after mixed and motor nerve repair with processed nerve allograft, Plast. Reconstr. Surg. Glob. Open 7 (2019) e2163, doi:10.1097/GOX.00000000000002163.
 [8] H.K. Frost, T. Andersson, S. Johansson, U. Englund-Johansson, P. Ekström,
- [8] H.K. Frost, T. Andersson, S. Johansson, U. Englund-Johansson, P. Ekström, L.B. Dahlin, F. Johansson, Electrospun nerve guide conduits have the potential to bridge peripheral nerve injuries in vivo, Sci. Rep. 8 (2018) 16716, doi:10.1038/s41598-018-34699-8.
- [9] S. Stojanov, A. Berlec, Electrospun nanofibers as carriers of microorganisms, stem cells, proteins, and nucleic acids in therapeutic and other applications, Front. Bioeng. Biotechnol. 8 (2020) 130, doi:10.3389/fbioe.2020.00130.
- [10] N. Ghane, S. Khalili, S. Nouri Khorasani, R. Esmaeely Neisiany, O. Das, S. Ramakrishna, Regeneration of the peripheral nerve via multifunctional electrospun scaffolds, J. Biomed. Mater. Res. A 109A (2021) 437–452, doi:10.1002/jbm.a.37092.
- [11] S. Lee, G. Jin, J.-H. Jang, Electrospun nanofibers as versatile interfaces for efficient gene delivery, J. Biol. Eng. 8 (2014) 30, doi:10.1186/1754-1611-8-30.
- [12] D.L. Puhl, D. Mohanraj, D.W. Nelson, R.J. Gilbert, Designing electrospun fiber platforms for efficient delivery of genetic material and genome editing tools, Adv. Drug Deliv. Rev. 183 (2022) 114161, doi:10.1016/j.addr.2022.114161.
- [13] A.M. Sandoval-Castellanos, F. Claeyssens, J.W. Haycock, Biomimetic surface delivery of NGF and BDNF to enhance neurite outgrowth, Biotechnol. Bioeng. 117 (2020) 3124–3135, doi:10.1002/bit.27466.
- [14] R. Li, Y. Li, Y. Wu, Y. Zhao, H. Chen, Y. Yuan, K. Xu, H. Zhang, Y. Lu, J. Wang, X. Li, X. Jia, J. Xiao, Heparin-poloxamer thermosensitive hydrogel loaded with bFGF and NGF enhances peripheral nerve regeneration in diabetic rats, Biomaterials 168 (2018) 24–37, doi:10.1016/j.biomaterials.2018.03.044.
- [15] S.J. Taylor, J.W. McDonald, S.E. Sakiyama-Elbert, Controlled release of neurotrophin-3 from fibrin gels for spinal cord injury, J. Control. Release 98 (2004) 281–294, doi:10.1016/j.jconrel.2004.05.003.
- [16] S.J. Taylor, E.S. Rosenzweig, J.W. McDonald, S.E. Sakiyama-Elbert, Delivery of neurotrophin-3 from fibrin enhances neuronal fiber sprouting after spinal cord injury, J. Control. Release 113 (2006) 226–235, doi:10.1016/j.jconrel.2006. 05.005
- [17] G.D. Sterne, R.A. Brown, C.J. Green, G. Terenghi, Neurotrophin-3 delivered locally via fibronectin mats enhances peripheral nerve regeneration, Eur. J. Neurosci. 9 (1997) 1388–1396, doi:10.1111/j.1460-9568.1997.tb01493.x.
- [18] G.D. Sterne, G.R. Coulton, R.A. Brown, C.J. Green, G. Terenghi, Neurotrophin-3enhanced nerve regeneration selectively improves recovery of muscle fibers expressing myosin heavy chains 2b, J. Cell Biol. 139 (1997) 709–715, doi:10. 1083/jcb.139.3.709.
- [19] A.M. Sandoval-Castellanos, F. Claeyssens, J.W. Haycock, Bioactive 3D scaffolds for the delivery of NGF and BDNF to improve nerve regeneration, Front. Mater. 8 (2021) 734683, doi:10.3389/fmats.2021.734683.
- [20] M.-H. Hong, H.J. Hong, H. Pang, H.-J. Lee, S. Yi, W.-G. Koh, Controlled release of growth factors from multilayered fibrous scaffold for functional recoveries in crushed sciatic nerve, ACS Biomater. Sci. Eng. 4 (2018) 576–586, doi:10. 1021/acsbiomaterials.7b00801.
- [21] D. Wu, Y. Zhang, X. Xu, T. Guo, D. Xie, R. Zhu, S. Chen, S. Ramakrishna, L. He, RGD/TAT-functionalized chitosan-graft-PEI-PEG gene nanovector for sustained delivery of NT-3 for potential application in neural regeneration, Acta Biomater. 72 (2018) 266–277, doi:10.1016/j.actbio.2018.03.030.
- [22] C. Liu, X. Li, F. Xu, H. Cong, Z. Li, Y. Song, M. Wang, Spatio-temporal release of NGF and GDNF from multi-layered nanofibrous bicomponent electrospun scaffolds, J. Mater. Sci. Mater. Med. 29 (2018) 102, doi:10.1007/ s10856-018-6105-x.
- [23] R. Klein, V. Nanduri, S. Jing, F. Lamballe, P. Tapley, S. Bryant, C. Cordon-Cardo, K.R. Jones, L.F. Reichardt, M. Barbacid, The trkB tyrosine protein kinase is a receptor for brain-derived neurotrophic factor and neurotrophin-3, Cell 66 (1991) 395–403, doi:10.1016/0092-8674(91)90628-C.
- [24] F. Lamballe, R. Klein, M. Barbacid, trkC, a new member of the trk family of tyrosine protein kinases, is a receptor for neurotrophin-3, Cell 66 (1991) 967– 979, doi:10.1016/0092-8674(91)90442-2.
- [25] C. Cordon-Cardo, P. Tapley, S. Jing, V. Nanduri, E. O'Rourke, F. Lamballe, K. Kovary, R. Klein, K.R. Jones, L.F. Reichardt, M. Barbacid, The trk tyrosine protein kinase mediates the mitogenic properties of nerve growth factor and neurotrophin-3, Cell 66 (1991) 173–183, doi:10.1016/0092-8674(91)90149-S.
- [26] B.J. Manadas, C.V. Melo, J.R. Gomes, C.B. Duarte, Neurotrophin signaling and cell survival, in: J.O. Malva, A.C. Rego, R.A. Cunha, C.R. Oliveira (Eds.), Interaction Between Neurons and Glia in Aging and Disease, Springer US, Boston, MA, 2007, pp. 137–172, doi:10.1007/978-0-387-70830-0_7.

- [27] D. Santos, F. Gonzalez-Perez, X. Navarro, J. del Valle, Dose-dependent differential effect of neurotrophic factors on in vitro and in vivo regeneration of motor and sensory neurons, Neural Plast. 2016 (2016) 4969523, doi:10.1155/ 2016/4969523
- [28] P.A. Dijkhuizen, W.T.J.M.C. Hermens, M.A.T. Teunis, J. Verhaagen, Adenoviral vector-directed expression of neurotrophin-3 in rat dorsal root ganglion explants results in a robust neurite outgrowth response, J. Neurobiol. 33 (1997) 172–184, doi:10.1002/(SICI)1097-4695(199708)33:2<172::AID-NEU6>3. 0.CO:2-#.
- [29] J. Yamauchi, J.R. Chan, E.M. Shooter, Neurotrophin 3 activation of TrkC induces Schwann cell migration through the c-Jun N-terminal kinase pathway, Proc. Natl. Acad. Sci. 100 (2003) 14421–14426, doi:10.1073/pnas.2336152100.
- [30] J.R. Chan, J.M. Cosgaya, Y.J. Wu, E.M. Shooter, Neurotrophins are key mediators of the myelination program in the peripheral nervous system, Proc. Natl Acad. Sci. 98 (2001) 14661–14668, doi:10.1073/pnas.251543398.
- [31] F. Hory-Lee, M. Russell, R.M. Lindsay, E. Frank, Neurotrophin 3 supports the survival of developing muscle sensory neurons in culture, Proc. Natl Acad. Sci. 90 (1993) 2613–2617, doi:10.1073/pnas.90.7.2613.
- [32] M.J. Groves, S.F. An, B. Giometto, F. Scaravilli, Inhibition of sensory neuron apoptosis and prevention of loss by NT-3 administration following axotomy, Exp. Neurol. 155 (1999) 284–294, doi:10.1006/expr.1998.6985.
- [33] L.-T. Kuo, A. Simpson, A. Schänzer, J. Tse, S.-F. An, F. Scaravilli, M.J. Groves, Effects of systemically administered NT-3 on sensory neuron loss and nestin expression following axotomy, J. Comp. Neurol. 482 (2005) 320–332, doi:10. 1002/cne.20400.
- [34] M.S. Ramer, I. Duraisingam, J.V. Priestley, S.B. McMahon, Two-tiered inhibition of axon regeneration at the dorsal root entry zone, J. Neurosci. 21 (2001) 2651–2660, doi:10.1523/JNEUROSCI.21-08-02651.2001.
- [35] Z. Sahenk, H.N. Nagaraja, B.S. McCracken, W.M. King, M.L. Freimer, J.M. Cedarbaum, J.R. Mendell, NT-3 promotes nerve regeneration and sensory improvement in CMT1A mouse models and in patients, Neurology 65 (2005) 681–689, doi:10.1212/01.WNL.0000171978.70849.c5.
- [36] Z. Sahenk, G. Galloway, K.R. Clark, V. Malik, L.R. Rodino-Klapac, B.K. Kaspar, L. Chen, C. Braganza, C. Montgomery, J.R. Mendell, AAV1.NT-3 gene therapy for Charcot-Marie-Tooth neuropathy, Mol. Ther. 22 (2014) 511–521, doi:10. 1038/mt.2013.250.
- [37] Z. Sahenk, J. Oblinger, C. Edwards, Neurotrophin-3 deficient Schwann cells impair nerve regeneration, Exp. Neurol. 212 (2008) 552–556, doi:10.1016/j. expneurol.2008.04.015.
- [38] A.T. Hanna-mitchell, D. O'leary, M.S. Mobarak, M.S. Ramer, S.B. Mcmahon, J.V. Priestley, E.N. Kozlova, H. Aldskogius, P. Dockery, J.P. Fraher, The impact of neurotrophin-3 on the dorsal root transitional zone following injury, Spinal Cord. 46 (2008) 804–810, doi:10.1038/sc.2008.57.
- [39] S. Hou, L. Nicholson, E. van Niekerk, M. Motsch, A. Blesch, Dependence of regenerated sensory axons on continuous neurotrophin-3 delivery, J. Neurosci. 32 (2012) 13206–13220, doi:10.1523/JNEUROSCI.5041-11.2012.
- [40] J.F. Poduslo, G.L. Curran, Permeability at the blood-brain and blood-nerve barriers of the neurotrophic factors: NGF, CNTF, NT-3, BDNF, Mol. Brain Res. 36 (1996) 280–286, doi:10.1016/0169-328X(95)00250-V.
- [41] H. Chen, Y. Xing, L. Xia, Z. Chen, S. Yin, J. Wang, AAV-mediated NT-3 overexpression protects cochleae against noise-induced synaptopathy, Gene Ther. 25 (2018) 251–259, doi:10.1038/s41434-018-0012-0.
- [42] C. Peng, X. Yin, M. Li, T. He, G. Li, Construction of a eukaryotic expression plasmid for human retina-derived neurotrophin-3, Neural Regen. Res. 8 (2013) 1031–1040, doi:10.3969/j.issn.1673-5374.2013.11.009.
- [43] J. Yang, S. Wu, L. Hou, D. Zhu, S. Yin, G. Yang, Y. Wang, Therapeutic effects of simultaneous delivery of nerve growth factor mRNA and protein via exosomes on cerebral ischemia, Mol. Ther. Nucleic Acids 21 (2020) 512–522, doi:10.1016/j.omtn.2020.06.013.
- [44] H. Steinle, J. Weber, S. Stoppelkamp, K. Große-Berkenbusch, S. Golombek, M. Weber, T. Canak-Ipek, S.-M. Trenz, C. Schlensak, M. Avci-Adali, Delivery of synthetic mRNAs for tissue regeneration, Adv. Drug Deliv. Rev. 179 (2021) 114007, doi:10.1016/j.addr.2021.114007.
- [45] Y. Fukushima, S. Uchida, H. Imai, H. Nakatomi, K. Kataoka, N. Saito, K. Itaka, Treatment of ischemic neuronal death by introducing brain-derived neurotrophic factor mRNA using polyplex nanomicelle, Biomaterials 270 (2021) 120681, doi:10.1016/j.biomaterials.2021.120681.
- [46] S.T. Crowley, Y. Fukushima, S. Uchida, K. Kataoka, K. Itaka, Enhancement of motor function recovery after spinal cord injury in mice by delivery of brainderived neurotrophic factor mRNA, Mol. Ther. Nucleic Acids 17 (2019) 465– 476, doi:10.1016/j.omtn.2019.06.016.
- [47] U. Sahin, K. Karikó, Ö. Türeci, mRNA-based therapeutics-developing a new class of drugs, Nat. Rev. Drug Discov. 13 (2014) 759–780, doi:10.1038/ nrd4278.
- [48] D.J. Williams, H.L. Puhl, S.R. Ikeda, A simple, highly efficient method for heterologous expression in mammalian primary neurons using cationic lipid-mediated mRNA transfection, Front. Neurosci. 4 (2010) 181, doi:10.3389/fnins. 2010.00181.
- [49] R. Goswami, G. Subramanian, L. Silayeva, I. Newkirk, D. Doctor, K. Chawla, S. Chattopadhyay, D. Chandra, N. Chilukuri, V. Betapudi, Gene therapy leaves a vicious cycle, Front. Oncol. 9 (2019) 297, doi:10.3389/fonc.2019.00297.
- [50] S. Patel, A. Athirasala, P.P. Menezes, N. Ashwanikumar, T. Zou, G. Sahay, LE. Bertassoni, Messenger RNA delivery for tissue engineering and regenerative medicine applications, Tissue Eng. Part A 25 (2019) 91–112, doi:10.1089/ ten.tea.2017.0444.

- [51] R.W. Malone, P.L. Felgner, I.M. Verma, Cationic liposome-mediated RNA transfection, Proc Natl Acad Sci USA 86 (1989) 6077–6081, doi:10.1073/pnas.86.16. 6077
- [52] M.A. Islam, E.K.G. Reesor, Y. Xu, H.R. Zope, B.R. Zetter, J. Shi, Biomaterials for mRNA delivery, Biomater. Sci. 3 (2015) 1519–1533, doi:10.1039/C5BM00198F.
- [53] H. Debus, P. Baumhof, J. Probst, T. Kissel, Delivery of messenger RNA using poly(ethylene imine)-poly(ethylene glycol)-copolymer blends for polyplex formation: Biophysical characterization and in vitro transfection properties, J. Control. Release 148 (2010) 334-343, doi:10.1016/j.jconrel.2010.09.007.
- [54] Z. Sharifnia, M. Bandehpour, H. Hamishehkar, N. Mosaffa, B. Kazemi, N. Zarghami, In-vitro transcribed mRNA delivery using PLGA/PEI nanoparticles into human monocyte-derived dendritic cells, Iran. J. Pharm. Res. 18 (2019) 1659–1675, doi:10.22037/ijpr.2019.1100872.
- [55] K. Karikó, H. Muramatsu, F.A. Welsh, J. Ludwig, H. Kato, S. Akira, D. Weissman, Incorporation of pseudouridine into mRNA yields superior nonimmunogenic vector with increased translational capacity and biological stability, Mol. Ther. 16 (2008) 1833–1840, doi:10.1038/mt.2008.200.
- [56] K. Karikó, M. Buckstein, H. Ni, D. Weissman, Suppression of RNA recognition by toll-like receptors: the impact of nucleoside modification and the evolutionary origin of RNA, Immunity 23 (2005) 165–175, doi:10.1016/j.immuni. 2005.06.008.
- [57] A. Wadhwa, A. Aljabbari, A. Lokras, C. Foged, A. Thakur, Opportunities and challenges in the delivery of mRNA-based vaccines, Pharmaceutics 12 (2020) 102, doi:10.3390/pharmaceutics12020102.
- [58] L.H. Nguyen, M. Gao, J. Lin, W. Wu, J. Wang, S.Y. Chew, Three-dimensional aligned nanofibers-hydrogel scaffold for controlled non-viral drug/gene delivery to direct axon regeneration in spinal cord injury treatment, Sci. Rep. 7 (2017) 42212, doi:10.1038/srep42212.
- [59] N. Zhang, J. Lin, V.P.H. Lin, U. Milbreta, J.S. Chin, E.G.Y. Chew, M.M. Lian, J.N. Foo, K. Zhang, W. Wu, S.Y. Chew, A 3D fiber-hydrogel based non-viral gene delivery platform reveals that microRNAs promote axon regeneration and enhance functional recovery following spinal cord injury, Adv. Sci. 8 (2021) 2100805, doi:10.1002/advs.202100805.
- [60] K. Xi, Y. Gu, J. Tang, H. Chen, Y. Xu, L. Wu, F. Cai, L. Deng, H. Yang, Q. Shi, W. Cui, L. Chen, Microenvironment-responsive immunoregulatory electrospun fibers for promoting nerve function recovery, Nat. Commun. 11 (2020) 4504, doi:10.1038/s41467-020-18265-3.
- [61] N. Zhang, U. Milbreta, J.S. Chin, C. Pinese, J. Lin, H. Shirahama, W. Jiang, H. Liu, R. Mi, A. Hoke, W. Wu, S.Y. Chew, Biomimicking fiber scaffold as an effective in vitro and in vivo microRNA screening platform for directing tissue regeneration, Adv. Sci. 6 (2019) 1800808, doi:10.1002/advs.201800808.
- [62] H.B. Wang, M.E. Mullins, J.M. Cregg, A. Hurtado, M. Oudega, M.T. Trombley, R.J. Gilbert, Creation of highly aligned electrospun poly-L-lactic acid fibers for nerve regeneration applications, J. Neural Eng. 6 (2009) 016001, doi:10.1088/ 1741-2560/6/1/016001.
- [63] A. Hurtado, J.M. Cregg, H.B. Wang, D.F. Wendell, M. Oudega, R.J. Gilbert, J.W. McDonald, Robust CNS regeneration after complete spinal cord transection using aligned poly-l-lactic acid microfibers, Biomaterials 32 (2011) 6068– 6079, doi:10.1016/j.biomaterials.2011.05.006.
- [64] S.-D. Yoon, Y.-S. Kwon, K.-S. Lee, Biodegradation and biocompatibility of poly l-lactic acid implantable mesh, Int. Neurourol. J. 21 (2017) S48–S54, doi:10. 5213/inj.1734882.441.
- [65] W.C. Low, P.-O. Rujitanaroj, D.-K. Lee, J. Kuang, P.B. Messersmith, J.K.Y. Chan, S.Y. Chew, Mussel-inspired modification of nanofibers for REST siRNA delivery: Understanding the effects of gene-silencing and substrate topography on human mesenchymal stem cell neuronal commitment, Macromol. Biosci. 15 (2015) 1457–1468, doi:10.1002/mabi.201500101.
- [66] W.H. Chooi, W. Ong, A. Murray, J. Lin, D. Nizetic, S.Y. Chew, Scaffold mediated gene knockdown for neuronal differentiation of human neural progenitor cells, Biomater. Sci. 6 (2018) 3019–3029, doi:10.1039/C8BM01034J.
- [67] H.J. Diao, W.C. Low, U. Milbreta, Q.R. Lu, S.Y. Chew, Nanofiber-mediated microRNA delivery to enhance differentiation and maturation of oligodendroglial precursor cells, J. Control. Release 208 (2015) 85–92, doi:10.1016/j. jconrel.2015.03.005.
- [68] H.J. Diao, W.C. Low, Q.R. Lu, S.Y. Chew, Topographical effects on fiber-mediated microRNA delivery to control oligodendroglial precursor cells development, Biomaterials 70 (2015) 105–114, doi:10.1016/j.biomaterials.2015.08.029
- [69] C. Pinese, J. Lin, U. Milbreta, M. Li, Y. Wang, K.W. Leong, S.Y. Chew, Sustained delivery of siRNA/mesoporous silica nanoparticle complexes from nanofiber scaffolds for long-term gene silencing, Acta Biomater. 76 (2018) 164–177, doi:10.1016/j.actbio.2018.05.054.
- [70] J.S. Chin, W.H. Chooi, H. Wang, W. Ong, K.W. Leong, S.Y. Chew, Scaffold-mediated non-viral delivery platform for CRISPR/Cas9-based genome editing, Acta Biomater. 90 (2019) 60–70, doi:10.1016/j.actbio.2019.04.020.
- [71] P. Wang, C. Zhang, Y. Zou, Y. Li, H. Zhang, Immobilization of lysozyme on layer-by-layer self-assembled electrospun nanofibers treated by post-covalent crosslinking, Food Hydrocoll. 121 (2021) 106999, doi:10.1016/j.foodhyd.2021. 106999
- [72] D.W. Nelson, D.L. Puhl, J.L. Funnell, U. Kruger, R.J. Gilbert, Multivariate analysis reveals topography dependent relationships amongst neurite morphological features from dorsal root ganglia neurons, J. Neural Eng. 19 (2022) 036026, doi:10.1088/1741-2552/ac7078.
- [73] J.S. McLane, N.J. Schaub, R.J. Gilbert, L.A. Ligon, Electrospun nanofiber scaffolds for investigating cell-matrix adhesion, in: A.S. Coutts (Ed.), Adhesion Protein Protocols, Third Edition, Humana Press, Totowa, NJ, 2013, pp. 371–388.

- [74] H. Kanno, Y. Pressman, A. Moody, R. Berg, E.M. Muir, J.H. Rogers, H. Ozawa, E. Itoi, D.D. Pearse, M.B. Bunge, Combination of engineered Schwann cell grafts to secrete neurotrophin and chondroitinase promotes axonal regeneration and locomotion after spinal cord injury, J. Neurosci. 34 (2014) 1838– 1855. doi:10.1523/INEUROSCI.2661-13.2014.
- [75] J.P. Brockes, K.L. Fields, M.C. Raff, Studies on cultured rat Schwann cells. I. Establishment of purified populations from cultures of peripheral nerve, Brain Res. 165 (1979) 105–118, doi:10.1016/0006-8993(79)90048-9.
- [76] T. Takami, M. Oudega, M.L. Bates, P.M. Wood, N. Kleitman, M.B. Bunge, Schwann cell but not olfactory ensheathing glia transplants improve hindlimb locomotor performance in the moderately contused adult rat thoracic spinal cord, J. Neurosci. 22 (2002) 6670–6681, doi:10.1523/JNEUROSCI.22-15-06670. 2002
- [77] A.R. D'Amato, D.L. Puhl, A.M. Ziemba, C.D.L. Johnson, J. Doedee, J. Bao, R.J. Gilbert, Exploring the effects of electrospun fiber surface nanotopography on neurite outgrowth and branching in neuron cultures, PLoS One 14 (2019) e0211731, doi:10.1371/journal.pone.0211731.
- [78] K.R. Jessen, R. Mirsky, The repair Schwann cell and its function in regenerating nerves, J. Physiol. 594 (2016) 3521–3531, doi:10.1113/JP270874.
- [79] K.R. Jessen, R. Mirsky, The success and failure of the Schwann cell response to nerve injury, Front. Cell. Neurosci. 13 (2019) 33, doi:10.3389/fncel.2019.00033.
- [80] C.R. Carvalho, J.M. Oliveira, R.L. Reis, Modern trends for peripheral nerve repair and regeneration: beyond the hollow nerve guidance conduit, Front. Bioeng. Biotechnol. 7 (2019) 337, doi:10.3389/fbioe.2019.00337.
- [81] A.R. D'Amato, D.L. Puhl, S.A.T. Ellman, B. Balouch, R.J. Gilbert, E.F. Palermo, Vastly extended drug release from poly(pro-17β-estradiol) materials facilitates in vitro neurotrophism and neuroprotection, Nat. Commun. 10 (2019) 4830, doi:10.1038/s41467-019-12835-w.
- [82] H.B. Wang, M.E. Mullins, J.M. Cregg, C.W. McCarthy, R.J. Gilbert, Varying the diameter of aligned electrospun fibers alters neurite outgrowth and Schwann cell migration, Acta Biomater. 6 (2010) 2970–2978, doi:10.1016/j.actbio.2010. 02.020.
- [83] T.R. Damase, R. Sukhovershin, C. Boada, F. Taraballi, R.I. Pettigrew, J.P. Cooke, The limitless future of RNA therapeutics, Front. Bioeng. Biotechnol. 9 (2021) https://www.frontiersin.org/articles/10.3389/fbioe.2021.628137. (accessed July 27, 2022).
- [84] B. Baptista, R. Carapito, N. Laroui, C. Pichon, F. Sousa, mRNA, a revolution in biomedicine, Pharmaceutics 13 (2021) 2090, doi:10.3390/pharmaceutics13122090.
- [85] O. Chabanovska, A.-M. Galow, R. David, H. Lemcke, mRNA a game changer in regenerative medicine, cell-based therapy and reprogramming strategies, Adv. Drug. Deliv. Rev. 179 (2021) 114002, doi:10.1016/j.addr.2021.114002.
- [86] H. Kwon, M. Kim, Y. Seo, Y.S. Moon, H.J. Lee, K. Lee, H. Lee, Emergence of synthetic mRNA: in vitro synthesis of mRNA and its applications in regenerative medicine, Biomaterials 156 (2018) 172–193, doi:10.1016/j.biomaterials.2017.11.
- [87] R. Firdessa-Fite, R.J. Creusot, Nanoparticles versus dendritic cells as vehicles to deliver mRNA encoding multiple epitopes for immunotherapy, Mol. Ther. -Methods Clin. Dev. 16 (2020) 50–62, doi:10.1016/j.omtm.2019.10.015.
- [88] M. Avci-Adali, A. Behring, T. Keller, S. Krajewski, C. Schlensak, H.P. Wendel, Optimized conditions for successful transfection of human endothelial cells with in vitro synthesized and modified mRNA for induction of protein expression, J. Biol. Eng. 8 (2014) 8, doi:10.1186/1754-1611-8-8.
- [89] A. Wahane, A. Waghmode, A. Kapphahn, K. Dhuri, A. Gupta, R. Bahal, Role of lipid-based and polymer-based non-viral vectors in nucleic acid delivery for next-generation gene therapy, Molecules 25 (2020) 2866, doi:10.3390/molecules25122866.
- [90] W. Ho, M. Gao, F. Li, Z. Li, X.-Q. Zhang, X. Xu, Next-generation vaccines: nanoparticle-mediated DNA and mRNA delivery, Adv. Healthc. Mater. 10 (2021) 2001812, doi:10.1002/adhm.202001812.
- [91] S.H. Pun, A.S. Hoffman, Nucleic acid delivery, in: B.D. Ratner, A.S. Hoffman, F.J. Schoen, J.E. Lemons (Eds.), Biomaterials Science, Third Edition, Academic Press, 2013, pp. 1047–1054.
- [92] R. Zangi, J.B.F.N. Engberts, Physisorption of hydroxide ions from aqueous solution to a hydrophobic surface, J. Am. Chem. Soc. 127 (2005) 2272–2276, doi:10.1021/ja044426f.
- [93] C.S. Tian, Y.R. Shen, Structure and charging of hydrophobic material/water interfaces studied by phase-sensitive sum-frequency vibrational spectroscopy, Proc. Natl. Acad. Sci. USA 106 (2009) 15148–15153, doi:10.1073/pnas. 0901480106
- [94] Z. Zhao, Z. Xia, C. Liu, H. Huang, W. Ye, Green synthesis of Pd/Fe3O4 composite based on polyDOPA functionalized reduced graphene oxide for electrochemical detection of nitrite in cured food, Electrochim. Acta 256 (2017) 146–154, doi:10.1016/j.electacta.2017.09.185.
- [95] S.J. Kim, W.H. Park, Polydopamine- and polyDOPA-coated electrospun poly(vinyl alcohol) nanofibrous membranes for cationic dye removal, Polym. Test. 89 (2020) 106627, doi:10.1016/j.polymertesting.2020.106627.
- [96] H. Lee, J. Rho, P.B. Messersmith, Facile conjugation of biomolecules onto surfaces via mussel adhesive protein inspired coatings, Adv. Mater. 21 (2009) 431–434, doi:10.1002/adma.200801222.
- [97] H. Lee, S.M. Dellatore, W.M. Miller, P.B. Messersmith, Mussel-inspired surface chemistry for multifunctional coatings, Science 318 (2007) 426–430, doi:10. 1126/science.1147241.
- [98] M.E. Lynge, R. van der Westen, A. Postma, B. Städler, Polydopamine—a nature-inspired polymer coating for biomedical science, Nanoscale 3 (2011) 4916–4928, doi:10.1039/C1NR10969C.

- [99] N.J. Schaub, C.D. Johnson, B. Cooper, R.J. Gilbert, Electrospun fibers for spinal cord injury research and regeneration, J. Neurotrauma 33 (2015) 1405–1415, doi:10.1089/neu.2015.4165.
- [100] D.L. Puhl, J.L. Funnell, D.W. Nelson, M.K. Gottipati, R.J. Gilbert, Electrospun fiber scaffolds for engineering glial cell behavior to promote neural regeneration, Bioengineering 8 (2021) 4, doi:10.3390/bioengineering8010004.
- [101] Y. Kim, V.K. Haftel, S. Kumar, R.V. Bellamkonda, The role of aligned polymer fiber-based constructs in the bridging of long peripheral nerve gaps, Biomaterials 29 (2008) 3117–3127, doi:10.1016/j.biomaterials.2008.03.042.
- [102] Q. Wei, T. Becherer, S. Angioletti-Uberti, J. Dzubiella, C. Wischke, A.T. Neffe, A. Lendlein, M. Ballauff, R. Haag, Protein interactions with polymer coatings and biomaterials, Angew. Chem. Int. Ed. 53 (2014) 8004–8031, doi:10.1002/ anie.201400546.
- [103] E.A. Vogler, Structure and reactivity of water at biomaterial surfaces, Adv. Colloid Interface Sci. 74 (1998) 69–117, doi:10.1016/S0001-8686(97)00040-7.
- [104] C. Lee, S.-H. Kim, J.-H. Jang, S.-Y. Lee, Enhanced cell adhesion on a nanoembossed, sticky surface prepared by the printing of a DOPA-bolaamphiphile assembly ink. Sci. Rep. 7 (2017) 13797. doi:10.1038/s41598-017-14249-4
- assembly ink, Sci. Rep. 7 (2017) 13797, doi:10.1038/s41598-017-14249-4.

 [105] W.-G. La, S.H. Bhang, J.-Y. Shin, H.H. Yoon, J. Park, H.S. Yang, S.-H. Yu, Y.E. Sung, B.-S. Kim, 3.4-dihydroxy-L-phenylalanine as a cell adhesion molecule
 in serum-free cell culture, Biotechnol. Prog. 28 (2012) 1055–1060, doi:10.

 1002/btpr.1560.
- [106] H.M. Kowalczy, G. Nowak, M. Inkielman, L. Sto, E. Marciniak, The shape of cells adhering to sulfonated copolymer surfaces, Cell. Mol. Biol. Lett. 10 (2005) 91–99.
- [107] P. Alves, S. Pinto, P. Ferreira, J.-P. Kaiser, A. Bruinink, H.C. de Sousa, M.H. Gil, Improving cell adhesion: development of a biosensor for cell behaviour monitoring by surface grafting of sulfonic groups onto a thermoplastic polyurethane, J. Mater. Sci. Mater. Med. 25 (2014) 2017–2026, doi:10.1007/ s10856-014-5233-1.
- [108] J. Radhakrishnan, A.A. Kuppuswamy, S. Sethuraman, A. Subramanian, Topo-graphic cue from electrospun scaffolds regulate myelin-related gene expressions in Schwann cells, J. Biomed. Nanotechnol. 11 (2015) 512–521, doi:10.1166/ibn.2015.1921.
- [109] D. Li, X. Pan, B. Sun, T. Wu, W. Chen, C. Huang, Q. Ke, H.A. El-Hamshary, S.S. Al-Deyab, X. Mo, Nerve conduits constructed by electrospun P(LLA-CL) nanofibers and PLLA nanofiber yarns, J. Mater. Chem. B 3 (2015) 8823–8831, doi:10.1039/C5TB01402F.
- [110] C.M. Valmikinathan, J. Hoffman, X. Yu, Impact of scaffold micro and macro architecture on Schwann cell proliferation under dynamic conditions in a rotating wall vessel bioreactor, Mater. Sci. Eng. C Mater. Biol. Appl. 31 (2011) 22–29, doi:10.1016/j.msec.2010.04.001.
- [111] L. Jin, X. Zeng, M. Liu, Y. Deng, N. He, Current progress in gene delivery technology based on chemical methods and nano-carriers, Theranostics 4 (2014) 240–255, doi:10.7150/thno.6914.
- [112] L. Parhamifar, A.K. Larsen, A.Christy Hunter, T.L. Andresen, S.Moein Moghimi, Polycation cytotoxicity: a delicate matter for nucleic acid therapy—Focus on polyethylenimine, Soft Matter 6 (2010) 4001–4009, doi:10.1039/C000190B.
- [113] E. Fröhlich, The role of surface charge in cellular uptake and cytotoxicity of medical nanoparticles, Int. J. Nanomed. 7 (2012) 5577–5591, doi:10.2147/IJN.
- [114] A.F. Adler, K.W. Leong, Emerging links between surface nanotechnology and endocytosis: impact on nonviral gene delivery, Nano Today 5 (2010) 553–569, doi:10.1016/j.nantod.2010.10.007.
- [115] A. Mantz, A.K. Pannier, Biomaterial substrate modifications that influence cell-material interactions to prime cellular responses to nonviral gene delivery, Exp. Biol. Med. 244 (2019) 100–113, doi:10.1177/1535370218821060.
- [116] Y. Liu, C.K.K. Choi, H. Hong, Y. Xiao, M.L. Kwok, H. Liu, X.Y. Tian, C.H.J. Choi, Dopamine receptor-mediated binding and cellular uptake of polydopaminecoated nanoparticles, ACS Nano 15 (2021) 13871–13890, doi:10.1021/acsnano. 1c06081.
- [117] J. Yamauchi, Y. Miyamoto, A. Tanoue, E.M. Shooter, J.R. Chan, Ras activation of a Rac1 exchange factor, Tiam1, mediates neurotrophin-3-induced Schwann cell migration, Proc. Natl. Acad. Sci. USA 102 (2005) 14889–14894, doi:10. 1073/pnas.0507125102.
- [118] J. Yamauchi, J.R. Chan, Y. Miyamoto, G. Tsujimoto, E.M. Shooter, The neurotrophin-3 receptor TrkC directly phosphorylates and activates the nucleotide exchange factor Dbs to enhance Schwann cell migration, Proc. Natl Acad. Sci. 102 (2005) 5198–5203, doi:10.1073/pnas.0501160102.

- [119] D. Middlemas, Neurotrophin 3, in: S.J. Enna, D.B. Bylund (Eds.), XPharm: The Comprehensive Pharmacology Reference, Elsevier, New York, 2007, pp. 1–3, doi:10.1016/B978-008055232-3.62270-6.
- [120] M.E. Yalvac, W.D. Arnold, C. Braganza, L. Chen, J.R. Mendell, Z. Sahenk, AAV1.NT-3 gene therapy attenuates spontaneous autoimmune peripheral polyneuropathy, Gene Ther. 23 (2016) 95–102, doi:10.1038/gt.2015.67.
- [121] M.E. Yalvac, J. Amornvit, L. Chen, K.M. Shontz, S. Lewis, Z. Sahenk, AAV1.NT-3 gene therapy increases muscle fiber diameter through activation of mTOR pathway and metabolic remodeling in a CMT mouse model, Gene Ther. 25 (2018) 129–138, doi:10.1038/s41434-018-0009-8.
- [122] B. Ozes, M. Myers, K. Moss, J. Mckinney, A. Ridgley, L. Chen, S. Bai, C.K. Abrams, M.M. Freidin, J.R. Mendell, Z. Sahenk, AAV1.NT-3 gene therapy for X-linked Charcot-Marie-Tooth neuropathy type 1, Gene Ther. (2021), doi:10.1038/s41434-021-00231-3.
- [123] Z. Sahenk, B.O. Ak, Gene therapy to promote regeneration in Charcot-Marie-Tooth disease, Brain Res. 1727 (2020) 146533, doi:10.1016/j.brainres.2019. 146533.
- [124] Gene therapy needs a long-term approach, Nat. Med. 27 (2021) 563, doi:10. 1038/s41591-021-01333-6.
- [125] C.P. Venditti, Safety questions for AAV gene therapy, Nat. Biotechnol. 39 (2021) 24–26, doi:10.1038/s41587-020-00756-9.
- [126] Z. Yang, Y. Yang, Y. Xu, W. Jiang, Y. Shao, J. Xing, Y. Chen, Y. Han, Biomimetic nerve guidance conduit containing engineered exosomes of adipose-derived stem cells promotes peripheral nerve regeneration, Stem Cell Res. Ther. 12 (2021) 442, doi:10.1186/s13287-021-02528-x.
- [127] K. Zhang, W.H. Chooi, S. Liu, J.S. Chin, A. Murray, D. Nizetic, D. Cheng, S.Y. Chew, Localized delivery of CRISPR/dCas9 via layer-by-layer selfassembling peptide coating on nanofibers for neural tissue engineering, Biomaterials 256 (2020) 120225, doi:10.1016/j.biomaterials.2020.120225.
- [128] Q. Xie, L. Jia, H. Xu, X. Hu, W. Wang, J. Jia, Fabrication of core-shell PEI/pBMP2-PLGA electrospun scaffold for gene delivery to periodontal ligament stem cells, Stem Cells Int. 2016 (2016) 5385137, doi:10.1155/2016/ 5385137.
- [129] J. Jin, Q. Saiding, X. Wang, M. Qin, Y. Xiang, R. Cheng, W. Cui, X. Chen, Rapid extracellular matrix remodeling via gene-electrospun fibers as a "patch" for tissue regeneration, Adv. Funct. Mater. 31 (2021) 2009879, doi:10.1002/adfm. 202009879.
- [130] Y. Yang, T. Xia, F. Chen, W. Wei, C. Liu, S. He, X. Li, Electrospun fibers with plasmid bFGF polyplex loadings promote skin wound healing in diabetic rats, Mol. Pharmaceutics. 9 (2012) 48–58, doi:10.1021/mp200246b.
- [131] Y. Zheng, Y. Wu, Y. Zhou, J. Wu, X. Wang, Y. Qu, Y. Wang, Y. Zhang, Q. Yu, Photothermally activated electrospun nanofiber mats for high-efficiency surface-mediated gene transfection, ACS Appl. Mater. Interfaces 12 (2020) 7905–7914, doi:10.1021/acsami.9b20221.
- [132] S. Liu, F. Wu, S. Gu, T. Wu, S. Chen, S. Chen, C. Wang, G. Huang, T. Jin, W. Cui, B. Sarmento, L. Deng, C. Fan, Gene silencing via PDA/ERK2-siRNA-mediated electrospun fibers for peritendinous antiadhesion, Adv. Sci. 6 (2019) 1801217, doi:10.1002/advs.201801217.
- [133] F. Zhou, X. Jia, Y. Yang, Q. Yang, C. Gao, S. Hu, Y. Zhao, Y. Fan, X. Yuan, Nanofiber-mediated microRNA-126 delivery to vascular endothelial cells for blood vessel regeneration, Acta Biomater. 43 (2016) 303–313, doi:10.1016/j. actbio.2016.07.048.
- [134] F. Zhou, M. Wen, P. Zhou, Y. Zhao, X. Jia, Y. Fan, X. Yuan, Electrospun membranes of PELCL/PCL-REDV loading with miRNA-126 for enhancement of vascular endothelial cell adhesion and proliferation, Mater. Sci. Eng.: C 85 (2018) 37–46, doi:10.1016/j.msec.2017.12.005.
- [135] M. Wen, H. Yan, X. Shi, Y. Zhao, K. Wang, D. Kong, X. Yuan, Modulation of vascular endothelial cells under shear stress on electrospun membranes containing REDV and microRNA-126, Int. J. Polymeric Mater. Polymeric Biomater. 70 (2021) 1090–1099, doi:10.1080/00914037.2020.1785452.
- [136] M. Wen, F. Zhou, C. Cui, Y. Zhao, X. Yuan, Performance of TMC-g-PEG-VAPG/miRNA-145 complexes in electrospun membranes for target-regulating vascular SMCs, Colloids Surf. B 182 (2019) 110369, doi:10.1016/j.colsurfb.2019. 110369.
- [137] C. Cui, M. Wen, F. Zhou, Y. Zhao, X. Yuan, Target regulation of both VECs and VSMCs by dual-loading miRNA-126 and miRNA-145 in the bilayered electrospun membrane for small-diameter vascular regeneration, J. Biomed. Mater. Res. A 107A (2019) 371-382, doi:10.1002/jbm.a.36548.